



## Monitoring/Imaging and Regenerative Agents for Enhancing Tissue Engineering Characterization and Therapies

Daniela Y. Santiesteban, *University of Texas Austin*  
Kelsey Kubelick, *Georgia Institute of Technology*  
Kabir S. Dhada, *University of Texas Austin*  
Diego Dumani, *Georgia Institute of Technology*  
Laura Suggs, *University of Texas Austin*  
[Stanislav Emelianov](#), *Emory University*

---

**Journal Title:** Annals of Biomedical Engineering  
**Volume:** Volume 44, Number 3  
**Publisher:** Springer Verlag (Germany) | 2016-03-01, Pages 750-772  
**Type of Work:** Article | Post-print: After Peer Review  
**Publisher DOI:** 10.1007/s10439-015-1509-y  
**Permanent URL:** <https://pid.emory.edu/ark:/25593/rwz0f>

---

Final published version: <http://dx.doi.org/10.1007/s10439-015-1509-y>

### Copyright information:

© 2015, Biomedical Engineering Society.  
This is an Open Access work distributed under the terms of the Creative Commons Attribution-NonCommercial-NoDerivatives 4.0 International License (<http://creativecommons.org/licenses/by-nc-nd/4.0/>).



Accessed September 23, 2019 4:16 AM EDT



Published in final edited form as:

*Ann Biomed Eng.* 2016 March ; 44(3): 750–772. doi:10.1007/s10439-015-1509-y.

## Monitoring/Imaging and Regenerative Agents for Enhancing Tissue Engineering Characterization and Therapies

Daniela Y. Santiesteban<sup>1,3</sup>, Kelsey Kubelick<sup>2,3</sup>, Kabir S. Dhada<sup>1</sup>, Diego Dumani<sup>2,3</sup>, Laura Suggs<sup>1</sup>, and Stanislav Emelianov<sup>2,3</sup>

<sup>1</sup>Department of Biomedical Engineering, University of Texas at Austin, 107 W. Dean Keeton, BME Building, 1 University Station, C0800, Austin, TX 78712, USA

<sup>2</sup>School of Electrical and Computer Engineering, Georgia Institute of Technology, 777 Atlantic Drive NW, Atlanta, GA 30332, USA

<sup>3</sup>Wallace H. Coulter Department of Biomedical Engineering, Georgia Institute of Technology, Emory University School of Medicine, 313 Ferst Dr NW, Atlanta, GA 30332, USA

### Abstract

The past three decades have seen numerous advances in tissue engineering and regenerative medicine (TERM) therapies. However, despite the successes there is still much to be done before TERM therapies become commonplace in clinic. One of the main obstacles is the lack of knowledge regarding complex tissue engineering processes. Imaging strategies, in conjunction with exogenous contrast agents, can aid in this endeavor by assessing *in vivo* therapeutic progress. The ability to uncover real-time treatment progress will help shed light on the complex tissue engineering processes and lead to development of improved, adaptive treatments. More importantly, the utilized exogenous contrast agents can double as therapeutic agents. Proper use of these Monitoring/Imaging and Regenerative Agents (MIRAs) can help increase TERM therapy successes and allow for clinical translation. While other fields have exploited similar particles for combining diagnostics and therapy, MIRA research is still in its beginning stages with much of the current research being focused on imaging or therapeutic applications, separately. Advancing MIRA research will have numerous impacts on achieving clinical translations of TERM therapies. Therefore, it is our goal to highlight current MIRA progress and suggest future research that can lead to effective TERM treatments.

### Keywords

Regenerative medicine; Imaging contrast agents; Therapeutic agents; Multimodal tracking; *In vivo* imaging; *In vivo* tracking; Stem cells; Scaffold engineering; Real-time imaging

---

Address correspondence to Laura Suggs, Department of Biomedical Engineering, University of Texas at Austin, 107 W. Dean Keeton, BME Building, 1 University Station, C0800, Austin, TX 78712, USA and Stanislav Emelianov, Wallace H. Coulter Department of Biomedical Engineering, Georgia Institute of Technology, Emory University School of Medicine, 313 Ferst Dr NW, Atlanta, GA 30332, USA. suggs@mail.utexas.edu and emelian@mail.utexas.edu.  
Associate Editor Rebecca Kuntz-Willits oversaw the review of this article.

## INTRODUCTION

Tissue engineering and regenerative medicine (TERM) have been actively researched for over three decades.<sup>18</sup> TERM research's goal is to develop therapies that replace diseased or damaged tissue with healthy, functioning tissues. Treatments are often multifaceted and may include cells, biomolecules, biomaterials, and imaging aspects. Although TERM research has seen numerous advances in recent years these have been primarily for skin, cartilage, and other simple connective tissues. As a whole, the field has not yet lived up to its expectations in clinic.<sup>179</sup> Regeneration of more complex organs has proven problematic partly because the healing and remodeling process remains poorly understood. In order to advance treatment success, knowledge about therapeutic progress along with material and tissue changes must be uncovered in real-time. Traditionally, information on TERM treatments came from end point analysis, such as histology or tissue function restoration. Real-time, non-invasive monitoring of treatment progress may allow TERM treatments to realize their full potential.

In order to achieve this level of characterization, imaging strategies must be implemented. Imaging techniques have already helped with monitoring TERM therapies and recent progress is discussed elsewhere.<sup>5,127</sup> To gain more detail and functional information, introduction of exogenous contrast agents is essential. These agents can be used to track stem cells (SCs), assess scaffold integrity, and convey functional changes. Furthermore, many of these agents have the added benefit of providing therapy. Combining their therapeutic and imaging capabilities can enhance therapeutic outcomes and also allow real-time, continuous monitoring of treatments. Particles that double as Monitoring/Imaging and Regenerative Agents (MIRAs) may provide the necessary knowledge to achieve successful TERM therapies and their translation to clinic.

The use of MIRAs is still in its emerging stages. While a similar idea using multifunctional particles has been extensively explored for cancer applications, dubbed theranostic (therapy and diagnostic) agents,<sup>192</sup> the TERM field has not widely explored the dual role of MIRAs. Instead, much of the research remains independent, focusing on either the therapeutic or imaging/monitoring benefit. Recently, focus has shifted to studying synergistic capabilities of MIRAs, but their full potential remains to be discovered.

Our goal is to review the current stages of particle-based MIRAs and suggest future opportunities for investigation. Because the final goal of treatment is clinical utility, we will concentrate on clinically practical MIRAs and imaging modalities. Therefore, we will emphasize photoacoustic (PA), ultrasound (US), magnetic resonance imaging (MRI), X-ray, and nuclear imaging modalities, such as positron emission tomography (PET), and describe the use of silica, gold, iron oxide, carbon, and perfluorocarbon particles (PFCps) as MIRAs (Table 1). Although other MIRA possibilities, such as quantum dots and reporter-gene imaging agents demonstrate preclinical utility, they fall out of scope of this review as our focus is on particulate materials capable of deep imaging. Therefore, these are not included because quantum dots are restricted to optical detection techniques with shallow imaging depths, and reporter genes are molecular, not material-based MIRAs.

## GOLD NANOPARTICLES

Colloidal gold has been used for centuries in medical and aesthetic applications. Initially, colloidal gold was of interest for its red color, for example in the famous color-changing Lycurgus Cup and stained glass windows. Since then, the development of Mie theory in the early 1900s explained that the color relates to the surface plasmon band. Mie theory continues to provide theoretical framework to describe the optical properties of these nanoparticles.<sup>38</sup> Today, gold nanoparticles (AuNPs) continue to be widely explored for biomedical applications and are excellent MIRAs due to their stability, biocompatibility, ease of synthesis and functionalization, and tunable optical properties.<sup>38,147,192</sup> AuNPs can be synthesized in a variety of sizes and shapes, including cages, rods, and spheres.<sup>148,158</sup> Varying geometry allows fine-tuning of optical properties due to gold's plasmonic nature. This property, known as surface plasmon resonance (SPR), creates a unique optical signature specific to particle composition.<sup>38,192</sup> The SPR and high optical absorption make AuNPs attractive contrast agents for PA imaging.<sup>32,83,126,204</sup> In X-ray/computed tomography (CT), AuNPs are investigated as alternatives to gadolinium, barium, or iodine-based agents due to their longer circulation time and improved contrast.<sup>62,75</sup>

AuNP synthesis differs according to shape and size. Citrate reduction is a popular technique for making spheres, where varying the ratio of citrate to gold correlates with particle size.<sup>38,192</sup> Figure 1a from Nam *et al.* shows an example of a TEM image of 20 nm AuNPs.<sup>126</sup> Synthesis of other shapes require capping agents, for example cetyltrimethylammonium bromide (CTAB) in nanorod synthesis.<sup>192</sup> Though nanorods are favored for PA imaging, CTAB is highly toxic, and additional protective layers and careful purification is required, especially for TERM applications.<sup>1</sup> For functionalization, thiolated biomolecules easily bind to the particle surface.<sup>192</sup>

### AuNPs as MIRAs

Since AuNPs are cytocompatible, do not negatively impact cell differentiation, and are easily taken up by cells *via* receptor-mediated endocytosis, they are of great interest for cell tracking applications.<sup>30,147</sup> While AuNPs can be used with optical imaging modalities to track SCs, we emphasize their use with X-ray/CT and PA/US due to greater imaging depth and clinical translatability. *In vivo* experiments using CT can provide migratory information. For example, AuNP-labeled mesenchymal stem cells (MSCs) could be followed as they migrated to a brain tumor.<sup>116</sup> Gold nanocages (AuNCs), gold nanorods (AuNRs), and gold nanospheres (AuNSs) generate strong PA signals to track cell location and migration.<sup>83,126,204</sup> Although AuNSs typically absorb around 520 nm where penetration depth is limited, SPR coupling upon MSC endocytosis generates a strong PA signal and a sensing mechanism to know particles are within cells (Fig. 1b from Nam *et al.*).<sup>126</sup> Though this is useful for cell tracking, it is disadvantageous for imaging other TERM therapies, such as scaffold remodeling where AuNSs are too far apart to generate substantial signals. While AuNRs or AuNCs may be more favorable for TERM imaging, they are more difficult to synthesize, are less stable than spheres, and rods are toxic without rigorous purification or further coating.<sup>1,29,158</sup>

Though tracking cell location is useful for therapeutic optimization, collecting functional information, including proliferation, neovascularization, and immune response, is critical to future development of TERM therapies. Experiments using X-ray/CT show great sensitivity to cellular events. *In vitro* experiments using nano/microCT could follow individual cells and mitosis by detecting AuNP distribution between daughter cells.<sup>7</sup> CT can also evaluate tumor growth rate and cell doubling time from the AuNP loading concentration and changes in the X-ray attenuation coefficient.<sup>8</sup> These measures of proliferation could apply to SC divisions, survival, and therapy success. Although neovascularization can be detected through PA imaging of hemoglobin absorbance, it is difficult to detect and distinguish new vessels. Integrin-targeted gold nanobeacons (GNBs) were developed to target only nascent vasculature and generated strong, specific PA signals *in vivo*.<sup>135</sup> To assess immune response, interactions between macrophages and MSCs can be observed during wound healing with a dual labeling system. In one recent study, AuNR-labeled MSCs were implanted *in vivo* along with free PEGylated AuNSs. As macrophages infiltrated the area and endocytosed the spheres, macrophage signal increased and was distinct from the MSC signal, providing a time course between cellular traffic and wound healing events.<sup>148</sup> Given the complex cellular interactions in the wound healing environment, future development of multi-labeling systems could provide valuable insights for improved MIRAs and TERM therapies.

In many of the previous examples, AuNPs were passively delivered to cells, but the surface can be easily functionalized for targeting, multimodal imaging, and biomolecule, drug, or gene delivery. Cytokine coatings have shown beneficial effects on modulating inflammation, while vascular endothelial growth factor receptor (VEGFR), antioxidants, or heparin manipulate wound healing and angiogenesis.<sup>13,50,87,103</sup> The advantage of delivering biomolecules with AuNPs vs. biomolecules alone is enhanced delivery.<sup>103</sup> Other cell alterations can be induced using AuNPs for gene and drug delivery. Cages are especially well suited for this application. AuNCs covered with smart polymers or phase-changing materials can encapsulate drugs or genetic material. Upon an external trigger, such as temperature change, these materials shrink and release the payload.<sup>120</sup> Other recent studies deliver genetic material through surface coatings. For example, AuNRs linked with siRNA could cross the blood–brain barrier (BBB) and knockdown dopaminergic signaling.<sup>20</sup> This provides an excellent platform for treating neurodegenerative disorders. Several studies have also induced osteogenesis and neurogenesis in SCs using plasmid DNA (pDNA) sequences linked to AuNPs.<sup>95,125</sup> Based on the contrast capabilities of AuNPs, in the future many of these delivery systems can be combined with cell tracking immediately in proof-of-concept studies.

Beyond surface modifications, AuNPs inherently possess qualities to manipulate angiogenesis or differentiation.<sup>92,124,198</sup> When MSCs were incubated with osteogenic differentiation media and AuNPs, higher concentrations of AuNPs increased osteogenic and reduced adipogenic differentiation through mechanotransduction. Figure 1c from Yi *et al.* depicts the impact of AuNPs on alkaline phosphatase (ALP) expression.<sup>198</sup> Gold's ability to manipulate cellular response adds to its utility as a MIRA since AuNPs can impact parallel signaling pathways without additional surface modifications. This creates more potent TERM treatments while limiting unwanted side effects. However, the osteogenic and antiangiogenic qualities of AuNPs could be harmful in certain situations, such as

cardiovascular applications. This problem could be mitigated through appropriate functionalization, but more research is needed as their role as MIRAs develops.

The influence of AuNPs on mechanical signaling is further utilized in scaffolding. AuNPs can add patterning, electrical stimulation, or points for cell–matrix interactions. A silk + AuNP scaffold was developed to increase scaffold stiffness, introduce 3D nanotopography, and add adhesion sites. When seeded with MSCs, cell spreading and density increased compared to smooth scaffolds.<sup>35</sup> Another study demonstrated gold-coated collagen nanofibers improved mechanical stability of the scaffold.<sup>131</sup> Gold, conductive scaffolds can induce MSCs towards neural and cardiac lineages.<sup>131</sup> For cardiovascular engineering, electrical stimulation drastically improved tissue function, seen through increased connexin-43 expression, more contractions/minute, lower excitation thresholds, and/or better conductivity between cells.<sup>46,131,201</sup> Figure 1d from You *et al.* provides an example of improved cardiomyocyte response in scaffolds with AuNPs and electrical stimulation.<sup>201</sup> While some AuNP delivery systems could immediately expand to cell tracking, scaffold monitoring is more of a challenge. Though PA imaging can be used to evaluate changes in oxygen saturation and vasculature at the scaffold site, higher resolution is needed to observe deeper changes in scaffold structure *in vivo*.<sup>23</sup>

### Current Limitations

Before AuNPs can be further developed as MIRAs problems such as particle cost, clearance, and degradation need to be addressed. AuNPs are cytocompatible in short-term studies, but there are concerns regarding long-term toxicity since the particles do not degrade. This issue can be avoided using AuNPs less than 5 nm diameter to allow renal clearance, but in this size range the PA signal is weak and circulation time is extremely short, limiting utility as a contrast agent.<sup>31</sup> An alternative approach is biodegradable nanoclusters, composed of AuNSs small enough for clearance.<sup>200</sup> However, controlling the degradation process of nanoclusters poses another challenge. Besides toxicity, limitations on large particle degradation and clearance brings up contrast transfer issues, also common to other MIRAs. When a labeled cell dies and is cleared by macrophages, the AuNPs are also transferred to the macrophage. As a result, the macrophage mistakenly appears as a cell of interest, reducing the specificity of the signal. Though the dual labeling system described previously is a step in the right direction, further research is needed.<sup>148</sup> Until issues of long-term toxicity, clearance, and degradation are solved, clinical translation of AuNPs as MIRAs is hindered.

### Outlook

AuNPs have been widely used for TERM monitoring and therapy separately. Though their combined use is minimally explored, the current state of research shows foundations exist for their use as effective MIRAs. The inertness of Au and high AuNP cell uptake makes them adept cell trackers, ease of surface modification allows a range of therapeutic applications, and electrical properties add a unique role as scaffold enhancers. Many of the described systems have all the components for immediate testing in proof-of-concept experiments combining TERM therapy and imaging, particularly for simultaneous delivery and cell tracking applications. Compared to the other MIRAs reviewed, AuNPs are best

suiting for applications related to cell tracking with PA imaging. Though AuNPs provide strong X-ray/CT contrast and could have a unique role in delivering therapeutics while assessing bone regeneration, it seems there is much room for research using AuNPs for PA imaging. The structure of AuNPs offers a wide range of opportunities for tracking multiple cellular events, and this is not as straightforward for other MIRAs. Furthermore, the ease of combining AuNPs with siRNA, biomolecules, or drugs, is a clear route to simultaneous TERM therapy and monitoring. Overall, the future of gold MIRAs is bright, and solutions to better link monitoring and therapy may include multimodal imaging and designing gold MIRAs as nanosensors.

## IRON OXIDE NANOPARTICLES

Iron oxide nanoparticles (IONPs), also known as superparamagnetic iron oxide nanoparticles (SPIONs), are unique MIRAs due to their inherent magnetic properties. They respond to external magnetic field gradients, and upon removal there is no remnant magnetization. This is an important attribute that reduces risk of aggregation.<sup>60,185</sup> Imaging and delivery applications take advantage of IONPs' magnetic properties, while their biocompatibility and ease of controlling mobility make them attractive for a variety of TERM uses.<sup>187</sup>

The use of IONPs as MRI contrast agents was first reported almost four decades ago using dextran-coated magnetite particles with sizes from 5 to 20 nm in gel systems.<sup>128</sup> At the same time, the particles were being studied to enhance delivery of chemotherapeutic agents using external magnetic fields.<sup>189</sup> It was soon suggested that MRI could be used to follow *in vivo* distribution of these agents.<sup>130</sup> Since then, they have been widely used to reduce local  $T_2/T_2^*$  relaxation time and yield negative contrast in  $T_2$ -weighted images. Although capable of reducing  $T_1$  relaxation time, the effect is not as significant as that on  $T_2/T_2^*$  due to a high  $T_2/T_1$  relaxivity ratio.<sup>85,185</sup> Current IONP research has evolved to include therapeutic delivery roles, cell labeling, and magnetic hydrogels, highlighting their MIRA capabilities.

IONPs are commonly synthesized through chemical co-precipitation of iron oxides. Typically used iron oxides are maghemite ( $\gamma\text{-Fe}_2\text{O}_3$ ) and magnetite ( $\text{Fe}_3\text{O}_4$ ), which are biocompatible and approved for clinical use.<sup>51,184,187</sup> To synthesize,  $\text{Fe}^{2+}$  and  $\text{Fe}^{3+}$  ions are co-precipitated in an aqueous salt solution by addition of a base. Varying type of salts, ion ratio, and pH dictates geometry.<sup>60,99,113</sup> More information on co-precipitation and synthesis methods can be found in other sources.<sup>60,73,99,113</sup> Beyond basic synthesis techniques, surface modifications impact kinetics, reduce toxicity, prevent aggregation, and enable functionalization for therapeutic use. This is usually achieved with a hydrophilic polymer surface coating, such as polyethylene glycol (PEG), polyvinyl alcohol (PVA), poly(acrylic acid), poly(lactide-*co*-glycolide) (PLGA), poly(ethyleneimine) (PEI), or various polysaccharides like dextran, chitosan, and pullulan.<sup>10,60,109,113,184</sup>

### IONPs as MIRAs

Numerous studies have used IONPs in conjunction with MRI to monitor cell distribution *in vivo*. For MSC tracking, IONPs are bound to the cell membrane or taken up by cells through different surface modifications.<sup>10,164,166</sup> Studies show MSC labeling does not negatively

affect cell viability<sup>51</sup> or ability to differentiate, regenerate tissue, and self-renew.<sup>11,104,163</sup> IONPs can also be used to transport SCs and other therapeutic agents. Their transport and location has been monitored in the brain,<sup>26</sup> heart,<sup>68</sup> vasculature,<sup>149</sup> muscle,<sup>3,167</sup> and joints.<sup>80</sup> IONPs enhance accumulation of cells to a specific site when a static magnetic field is applied by placing external or implanted permanent magnets.<sup>26,149</sup> This effect can be confirmed with MRI (Fig. 2a from Talaie *et al.*).<sup>167</sup> Further studies of external magnet effects on therapeutic agent kinetics would help optimize and control their placement depending on monitored therapy outcome.

IONPs have also been used to deliver genetic material. Additional coatings like PEG,<sup>137</sup> lipid-like materials,<sup>77</sup> PEI, and chitosan,<sup>90</sup> allow pDNA loading onto a cluster of particles (Fig. 2b from Jiang *et al.*). Mesoporous IONPs provide increased carrier loading by utilizing both inner and outer cavities.<sup>25</sup> Loaded IONPs can then be incubated with cells prior to implantation, or delivered *via* an external magnetic field that guides clusters to the desired site. For example, one study used polypeptide-coated, fluorescently labeled IONPs to show *in vivo* transfection and tracking of MSCs using multimodal MR/optical imaging.<sup>138</sup> Magnetofection can enhance transfection by pulling the genes toward the target cells when an external magnetic field is applied.<sup>42,142</sup> A magnetofection study using PEG-coated IONPs crosslinked with vascular endothelial growth factor (VEGF) pDNA showed elevated VEGF production from rat MSCs for cerebral ischemia therapy (Fig. 2c from Plank *et al.*).<sup>137</sup> Another strategy is conjugating IONPs with ligands to enhance receptor-mediated endocytosis and increase treatment efficacy.<sup>104</sup> Mechanical and thermal stimulation with different magnetic field regimens would be an interesting area to study as it can affect MSC fate<sup>54,59</sup> and has not been thoroughly explored.

Alternative IONP-based delivery mechanisms involve loading them into hydrogels and controlling release of proteins or cells. While conventional scaffolds usually depend on passive release of cells and agents, IONPs enable control *via* magnetic stimulation that deforms or increases hydrogel temperature (Figs. 2d and 2e from Zhao *et al.*).<sup>70,106,118,205</sup> Other studies show magnetic scaffolds can reload IONP-labeled growth factors (GFs) and SCs through magnetic attraction. This technique allows for a higher degree of control during TERM therapies, compared to traditional approaches where agents must be preloaded before implantation,<sup>19</sup> and it could be used for long-term treatments that would otherwise be limited by the hydrogel environment. More studies on long-term outcomes are needed to elucidate the full potential of magnetic scaffolds.

IONPs are also studied as imaging agents in magneto-motive based modalities<sup>81,115,129</sup> and for combined MRI and nuclear imaging when IONPs are radiolabeled.<sup>40,102</sup> Magneto-motive modalities offer cost-efficient, localized monitoring. Combining MRI with nuclear imaging adds increased sensitivity while preserving spatial resolution of MRI. Although IONPs could serve as PA imaging agents, use of this modality would not be ideal because of their low absorption in the near infrared (NIR) which implies limited imaging depth.<sup>36</sup> Research on combined multimodal particles can potentially improve these capabilities.<sup>78</sup>

## Current Limitations

The fact that MRI is the most widely used modality to monitor IONP distribution means their use as MIRAs frequently shares this technology's limitations, including high cost, low sensitivity, and inability for real-time imaging. Another limitation of IONPs as MRI-based MIRAs is that their negative contrast makes detection difficult in dark, low-contrast regions.<sup>21,161</sup> To combat this issue, gadolinium-labeled IONPs have been investigated as a solution to increase both T1 (positive) and T2 contrast.<sup>9</sup> Other studies have been able to obtain positive contrast *in vivo* by modifying imaging sequences or applying post-processing algorithms.<sup>37,206</sup> Adding nuclear imaging could improve contrast and sensitivity limitations in a full-body image, while a technique like magneto-motive ultrasound could be used to closely examine a specific area in real-time. These additions would allow for more extensive TERM treatment monitoring.

In cell tracking studies, the loss of contrast resulting from cell division and transfer of nanoparticles to non-stem cells can lead to underestimation and overestimation, respectively.<sup>173,181</sup> Both issues limit accurate, long-term monitoring of therapy efficacy. *Ex vivo* experiments have revealed that IONPs from dead stem-cells are phagocytosed by macrophages, an effect otherwise indistinguishable on *in vivo* MRI.<sup>112,209</sup> Overestimation of cells could be improved with surface functionalization to reduce non-specific macrophage uptake<sup>193</sup> or by using additional agents to detect macrophages, similar to strategies with AuNPs.<sup>148</sup>

## Outlook

Iron oxide nanoparticles have demonstrated unique versatility as MIRAs. Their therapeutic capabilities include acting as cell trackers, gene delivery vehicles, and scaffold enhancers. The fact that they are superb MRI contrast agents and approved for clinical use allows for full body imaging and easy translation, and their ability to respond to magnetic fields adds interesting features when compared to other MIRAs. Magnetic delivery is thus a prominent application of IONPs. The use of nuclear imaging and magneto-motive techniques can improve monitoring by adding sensitivity and versatile real-time imaging. Challenges still remain to be able to identify SC quantity over time; however, synergistic use of IONPs and other agents, like AuNPs, could help distinguish SCs from macrophages while allowing use of static fields for cell guidance. IONPs have a promising future, be it as a single agent, multi-agent, or multimodal uses. Additional *in vivo* studies will help elucidate their roles as effective MIRAs.

## CARBON NANOTUBES

Carbon nanotubes (CNTs) are a subset of the fullerene carbon allotrope family. Although unintentionally observed around the 1960s, the official discovery of CNTs is credited to Iijima in 1991.<sup>74</sup> Since then, CNTs have been studied in a variety of applications including electronics, catalysts, sensors, and biomedical.<sup>133</sup> CNTs consist of single or multiple rolled up sheets of graphene and are called single-walled (SWCNTs) or multiple-walled (MWCNTs), respectively.<sup>197</sup> CNTs are characterized by long lengths and nanometer diameters leading to large aspect ratios. Their high surface area and ability to be strategically

functionalized, combined with their excellent mechanical and electrical properties, have led to a wide range of CNT applications, from drug/protein carriers to scaffold enhancers.<sup>44,65,145</sup> Additionally, CNTs act as contrast agents for clinically relevant imaging modalities such as PA, US, MRI, and nuclear imaging.<sup>39,41,186</sup> CNTs can act as contrast agents for different *in vitro* optical imaging techniques and Raman spectroscopy, but these features are discussed in other sources.<sup>56,71,108,110</sup>

Various studies demonstrate CNT ability to serve as T2-weighted contrast agents for MRI. Their T2 contrast arises from lingering iron atoms used during the nanotube synthesis and from the carbon material itself.<sup>2</sup> Addition of MRI contrast agents, such as IONPs or gadolinium, enhances CNT contrast abilities. Attaching IONPs to CNTs further increases T2 contrast,<sup>89</sup> while adsorption of gadolinium chelates to CNTs cause a contrast increase for both T1 and T2-weighted images.<sup>146</sup>

Bare CNTs show PA contrast when injected into mice<sup>39</sup> due to strong optical absorbance in the NIR region.<sup>86</sup> Functionalization of higher optically absorbing agents further increases contrast. For example, gold plated CNTs showed a 100 fold enhancement in signal,<sup>91</sup> while conjugation of indocyanine green (ICG) showed a 300 fold signal increase in *in vivo* studies (Fig. 3a from Zerda *et al.*).<sup>203</sup>

CNTs are commonly synthesized by chemical vapor deposition involving metal catalysts.<sup>65,84</sup> The metal remains on the formed nanotubes, raising concerns of cytotoxicity. However, appropriate purifying techniques, such as acid etching, remove the majority of metal atoms and simultaneously generate nanotube defects for functionalization points.<sup>65,192</sup> Functionalization of CNTs is essential as it reduces their tendency to aggregate and cytotoxicity through a reduction in hydrophobicity.<sup>188</sup> Appropriate techniques are discussed elsewhere.<sup>108,170,175</sup>

### CNTs as MIRAs

CNTs are attractive stem cell trackers because they are readily taken up by cells, and appropriate functionalization and dose show no adverse effect on MSC viability, proliferation, and differentiation potential.<sup>121,182</sup> One example of cell tracking was shown by pre-labeling MSCs with SWCNTs which allowed *in vivo* MRI and PA tracking.<sup>186</sup> As noted earlier, SC tracking is important for TERM applications to ensure implanted cells are at the desired location.

Due to high cell uptake, CNTs have also been explored to deliver TERM therapeutics. Their high surface area and design allows for immobilization of therapeutics through functional attachments, adsorption, or entrapment (Fig. 3b from Hirsch *et al.*).<sup>34,69</sup> The remaining hydrophobic portions of the CNTs are able to interact with cell membranes for efficient uptake.<sup>65</sup> If desired, CNTs can be functionalized with cationic polymers, such as PEI, to improve transfection capabilities.<sup>123</sup> For drug delivery, compounds with aromatic groups can easily link to CNTs through  $\pi$ - $\pi$  stacking.<sup>180</sup> Drugs can also bind to CNTs through amide or ester linkages to COO-groups present at CNT defect sites.<sup>192</sup> If specific cell targeting is required, CNTs can be functionalized with receptor-targeted ligands.<sup>180,186</sup>

PA/US techniques can control cargo release and monitor CNT location, highlighting their MIRA potential. In one study, *in vivo* US monitoring of MWCNTs was done in combination with targeted drug delivery.<sup>191</sup> Since CNTs absorb strongly in the NIR region, irradiation at these wavelengths can elicit changes to release cargo.<sup>86</sup> Other examples of controlled release include microcapsules, or spherical hydrogels, embedded with CNTs and the desired biomolecules.<sup>139,208</sup> Upon irradiation, CNTs convert the absorbed light into heat, thereby increasing membrane permeability or rupturing the capsule for cargo release. While the majority of these studies looked at cancer drug delivery, TERM therapies would benefit from similar controllable *in vivo* therapeutic delivery and monitoring. One can envision CNTs functionalized with different absorber-therapeutic pairs that can be selectively triggered based on irradiation wavelength. This would allow for controlled release of multiple therapeutics to enhance individual or synergistic TERM therapies.

Laser irradiation of CNTs alone has also shown TERM therapeutic benefits. NIR irradiation of CNTs cultured with MSCs provoked cells to release elevated levels of calcium, ALP, and osteopontin, indicating differentiation towards osteoblasts, as shown in Fig. 3c from Green *et al.*<sup>58</sup> Similarly, irradiation of CNTs within an alginate gel induced bone growth *in vivo*.<sup>195</sup> It is postulated that bone formation results from photothermal therapy triggered by the localized heating of CNTs following irradiation.

The diversity of CNTs as MIRAs is supported by their wide array of applications within scaffold engineering. Their hexagonal carbon network gives them lightweight, superior mechanical properties and unique electrical properties.<sup>122,175</sup> In bone TERM applications, incorporating CNTs into polymeric scaffolds increases mechanical strength.<sup>117,157</sup> For example, addition of CNTs into PLGA scaffolds improved the compressive strength and moduli two and three times, respectively, over PLGA scaffolds alone.<sup>117</sup> *In vivo* studies of CNT-based arrays or CNT scaffold composites demonstrate good cell attachment, proliferation, osteogenic differentiation, and integration.<sup>98,107,156</sup> CNTs also possess high electrical conductivity; consequently, they have been studied for neural and cardiac TERM applications.<sup>101,122</sup> Several *in vitro* studies have shown the ability of CNTs to direct neuronal growth and enhance signal transfer.<sup>101,152,202</sup> The success of these *in vitro* studies supports further exploration through *in vivo* studies. Integration of CNTs into scaffolds also allows for scaffold degradation and tissue ingrowth monitoring.<sup>22</sup> Groups have demonstrated the ability to use PA/US to monitor blood vessel ingrowth and scaffold location *ex vivo*<sup>24</sup> and *in vivo*.<sup>168</sup> This feature could benefit from future studies as longitudinal characterization of such parameters is important for monitoring angiogenic TERM therapy progress.

Lastly, CNTs have been investigated as various types of biosensors ranging from electrochemical to optical sensors. Optical CNT sensors can monitor levels of glucose and other signaling molecules, such as nitric oxide (NO).<sup>12,177</sup> NO signals vasodilation; therefore, monitoring NO levels could convey local changes of blood dynamics in response to TERM therapies. Unfortunately, the current technology of these applications relies on detecting CNT fluorescent changes upon molecule binding and therefore has limited sensing depths.<sup>196</sup> Studying alternative detection methods to increase depth-sensing capabilities or ways to relay information to an external monitor would be beneficial.

## Current Limitations

CNTs possess many unique properties that make them attractive MIRAs, but some of these same properties raise concerns for their use in medical applications. As of yet, CNTs are not FDA approved or in clinical trials. Their non-degradability leads to questions of biodistribution and persistence which remain to be properly answered.<sup>55</sup> As previously mentioned, functionalization of CNTs decreases cytotoxic side effects and also effects pharmacokinetics by decreasing CNT clearance time.<sup>55</sup> It appears CNT type, dose, and functionalization prove key in determining their biocompatibility. The TERM field would benefit from future studies to clearly identify and optimize the best form of CNTs for biomedical use to clarify discrepancies. For instance, several studies involving CNTs for tracking cells showed no cytotoxic or differentiation effects,<sup>44,121,182</sup> yet others have demonstrated CNTs negatively impact cell proliferation or differentiation.<sup>111</sup>

## Outlook

CNTs have clearly demonstrated their ability to act as effective MIRAs. Although CNTs show contrast in US, PA, and MRI applications, they are inherently best suited for PA applications. Bare CNTs show little US and MRI contrast and often have to be functionalized with other agents (i.e. IONPs). Additionally, CNT cargo can be triggered to release *via* PA techniques. Another interesting area for future exploration is CNT incorporation into scaffolds. CNTs have already demonstrated the ability to increase physical and conductive properties of scaffolds while allowing non-destructive characterization and monitoring of therapy progress. There is still much to be done to benefit from CNTs as MIRAs and expedite their path to clinical use, including investigating CNT parameter influence on biocompatibility and clearance.<sup>140</sup> Once this has been optimized, areas such as targeted/controlled drug delivery and longitudinal scaffold and tissue in-growth assessment could gain from CNT's unique properties.

## SILICA-BASED PARTICLES

Silica is a well-characterized biocompatible material with tunable parameters such as size, porosity, and surface chemistry. Silica-based nanoparticles fall into two predominant categories, mesoporous silica nanoparticles (MSNs) and solid silica nanoparticles (SiNPs) (Fig. 4a from Chen *et al.* and Vivero-Escot *et al.*). Material MCM-41 was discovered by the Mobil Corporation as a potential catalyst in 1992 and is the most commonly used in MSNs.<sup>16</sup> Its potential for biomedical applications was not researched until the early 2000s and has been rapidly investigated since then. Silica particles display ultrasound echogenicity, but are mostly used to incorporate a variety of imaging motifs due to their large surface area, porosity, and surface functionalization. Contrast agents are doped into silica particles for MRI, PET, and NIR fluorescence imaging. Functionalizing silica particles allows them to contain multiple contrast agents and deliver therapeutics for TERM applications. Additionally, silica-based particles have applications in scaffold engineering and cell monitoring.<sup>27,52,155</sup>

The most widely used silica nanoparticle synthesis method is the Stöber method developed by Stöber and co-workers in the 1960s.<sup>162</sup> The method consists of hydrolysis and

condensation of tetraethyl orthosilicate (TEOS) in ethanol and water, catalyzed by ammonia. This produces monodisperse spherical particles with size tuned by adjusting reaction conditions. An alternative is the reverse microemulsion method developed in the 1990s.<sup>6</sup> MSNs are synthesized using evaporation-induced self-assembly developed in 1992. For example, surfactant molecules are added to form a template that is later extracted post-silica polymerization, leaving behind pores.<sup>16,97</sup> MSNs can be functionalized on their external surface and within pores (Fig. 4b from Slowing *et al.*), and hollow MSNs provide more volume for particulate transport.<sup>169,211</sup> There are two main methods to alter surface chemistry: post-synthesis grafting or co-condensation of trialkoxysilanes during nanoparticle synthesis.<sup>160,171</sup> By altering surface chemistry to include peptides and antibodies, silica particles can target surface and intracellular markers.<sup>96</sup>

### Silica Particles as MIRAs

Silica particles are often used as contrast agents to monitor stem cell therapy due to silica's tunable and biocompatible properties. Inclusion of contrast agents allows *in vivo* visualization of SCs with US, MRI, and PET.<sup>72,82,88</sup> MSNs were investigated for guiding cardiac SC therapy injection using US. MSN-loaded MSCs were delivered into the left ventricle of a mouse model and could monitor injected cells (Fig. 4c from Zhou *et al.*). After one month, MSNs were degraded by intracellular pathways with little trace and no toxic effect, appealing qualities for clinical translation.<sup>88</sup> In conjunction with US, MRI has been used to monitor SCs *in vivo* by loading Gd-labeled SiNPs into MSCs. Particles could be imaged for up to 13 days, with the limiting factor being cell division dilution.<sup>82</sup> In another multimodal study, MSNs were functionalized with Cu, Gd, and a fluorophore, and implanted into MSCs for multimodal tracking using PET, MRI, and fluorescence. *In vivo* loading of the doped, MSN-labeled MSCs allowed tracking using PET and MRI simultaneously.<sup>72</sup> Silica particles' major strength is their ability to incorporate multiple contrast agents into a single element, which can provide numerous tracking options for clinicians in future applications.

Due to silica particles' surface functionalization, and specifically MSNs' porosity, silica is being investigated for drug and gene delivery.<sup>53,66,134</sup> MSNs undergo endocytosis in cells, including MSCs, with no adverse effect on differentiation, viability, and proliferation.<sup>33</sup> The large pore volume and surface area allows for nucleic acid, peptides, and polymers to be adsorbed, trapped, or bound.<sup>176</sup> This provides a multifunctional platform for controlled release and simultaneous sensing/imaging. MSNs showed the ability to transport membrane-impermeable proteins across cell membranes by trapping them within MSN pores and releasing them intracellularly.<sup>159</sup> MSNs have been used as carriers for peptide mimetics to drive embryonic stem cell differentiation into functional motor neurons *in vivo*, and the differentiated SCs displayed long-term survival.<sup>53</sup> MSNs' extensive carrying abilities should continue to be investigated for optimizing TERM therapeutic delivery.

Silica particles have tunable porosity, mechanical properties, and bioactivity that provide helpful tools for use in scaffolds. *In vitro* studies demonstrated SiNPs promote differentiation of MSCs into osteoblasts. This translated well *in vivo*, where SiNPs increased bone mineral density.<sup>15,61</sup> SiNPs/MSNs can interact especially well with the

musculoskeletal system, considering their frequent incorporation into bone tissue engineering scaffolds.<sup>52,105,144,210</sup> For instance, MSNs were embedded into a zein-hydroxypropyltrimethyl ammonium chloride chitosan (HACC) scaffold and implanted into a critical-sized radial bone defect in a rabbit model (Fig. 4d from Kempen *et al.*). The scaffold provided structure and enhanced osteogenic differentiation to regenerate the missing bone segment.<sup>210</sup> These results demonstrate the future clinical relevance and promise of silica particles as orthopedic regenerative biomaterials. MSNs embedded in poly(caprolactone) have been used in laser tissue soldering, a tissue fusion method, due to their uptake and retention of ICG. ICG is a photodynamic agent that absorbs energy upon irradiation and releases energy as heat, which induces tissue fusion. The MSNs retain ICG in the scaffold before, during, and after irradiation, allowing for a constant reproducible temperature increase. An *in vivo* study demonstrated successful rabbit aortic artery tissue fusion with little thermal damage and intact endothelium because MSNs controlled photodynamic agent movement and minimized cytotoxic effects.<sup>153</sup> Future investigation combining photodynamic heating agents and scaffolds using silica particles may be crucial to developing an all-encompassing therapy.

### Current Limitations

Silica-based nanoparticles are unable to act as effective MIRAs on their own due to inherently minimal contrast agent characteristics. Although they can be readily doped with other agents, incorporation requires a variety of chemical reactions, making it difficult to combine various particles for multi-modal imaging. Furthermore, adding various drugs or biomolecules for therapy can complicate development and limit which compounds bind to the silica. Combining separate contrast agents also raises concerns of leakage out of the system, causing reduced resolution and possible cytotoxicity. Another limitation is the large size of MSNs, which can limit cell uptake. Work is being done to reduce the size to sub-100nms and overcome this issue. Currently, silica nanoparticles are not FDA approved but are undergoing clinical trials for cancer therapy, which can be translated to tissue engineering in the future.<sup>141</sup> As research continues and these problems are solved, silica can begin to become a clinically viable MIRA.

### Outlook

The future of silica particles as MIRAs lies in continuing to investigate capabilities with combinations of contrast and therapeutic agents. Silica particles are readily taken up by cells and well known functionalization techniques make them efficient gene and drug delivery agents. Silica has useful chemical properties for tissue scaffold development, and its bioactivity can simultaneously enhance SC differentiation. Their well-investigated chemical modifications have made SiNPs effective contrast agent carriers. While silica nanoparticles display some contrast in US, they are better suited as a carrier for MRI or PET contrast agents. Silica-based particles can provide novel therapy through therapeutic delivery and monitoring while acting as a scaffold base. Its most current clinically viable application lies in treating orthopedic disease. There have been some studies combining their therapeutic ability and imaging potential, but more work must be done to reach clinical relevance. Further investigation into silica particles' ability to monitor SC therapy with viability

detection, scaffold engineering, and contrast agent cytotoxicity must be addressed prior to them becoming clinically relevant MIRAs.

## PERFLUOROCARBON PARTICLES

PFCps have a long history in biomedical applications ranging from use as liquid ventilators to US contrast agents. More recently PFCp research has expanded to exploit their potential as multi-functional agents in a variety of TERM applications. PFCps are most studied as therapeutic carriers, capable of delivering drugs, genes, GFs, and oxygen to cells and tissues. PFCps are attractive therapeutic deliverers because combining them with PA or US allows for controlled release and *in vivo* monitoring of TERM therapy delivery. Other TERM applications of PFCps are targeted molecular imaging and delivery and scaffold monitoring.

PFCps are typically synthesized with emulsion techniques or microfluidic devices (Fig. 5a from Duncanson *et al.*).<sup>45</sup> The encapsulating PFCp shells are synthesized from polymers, lipids, proteins, or a combination of the aforementioned.<sup>190</sup> Their perfluorocarbon (PFC) core can be gaseous or liquid, depending on the chosen PFC compound. Gaseous forms of PFCps are called nanobubbles or microbubbles (MBs) based on their nano or micron diameter, while liquid forms are called nanodroplets or microdroplets, again based on size.

MBs have been extensively investigated as US contrast agents and were clinically approved as echocardiography contrast agents in 1992.<sup>114</sup> Their gaseous core offers a drastic acoustic impedance mismatch between the surrounding tissue and biological fluids, making them superb US contrast agents.<sup>93</sup> The fact that some PFCps are already clinically approved further emphasizes their potential as clinically used MIRAs.

Nanodroplet (ND) PFCps have recently gained attention as multimodal contrast agents capable of reaching places larger MBs cannot.<sup>63,151</sup> Additionally, the use of ultrasound or laser irradiation can convert NDs into MBs for continued use as US contrast agents. US elicits phase change of droplets into bubbles through application of appropriate acoustic pressures, termed acoustic droplet vaporization (ADV).<sup>154</sup> Laser-induced phase change requires incorporating optical absorbers responsive to applied pulsed laser irradiation into NDs. Dyes (ICG, 1064 dye) and AuNRs were investigated as optical triggers for initiating phase transition from NDs to MBs.<sup>63,64,190</sup> Figure 5b from Hannah *et al.* shows ICG-loaded NDs and their PA/US contrast capabilities upon irradiation.<sup>63</sup> Droplet PFCps can also be monitored as *in vivo* <sup>19</sup>F MRI contrast agents due to their high fluorine concentrations.<sup>76</sup> Since fluorine is not present at high quantities in biological systems, the fluorine signal should only come from PFCps. This allows for high specificity of functional information which can then be combined with anatomical information gained through <sup>1</sup>H MRI.<sup>57</sup>

### PFCps as MIRAs

PFCps have been widely investigated as therapeutic delivery agents. Charged species, such as genes, are normally loaded through electrostatic interactions with cationic PFCps.<sup>4,79</sup> Cationic particles carry higher payloads of nucleic acids and better prevent premature degradation compared to neutral particles.<sup>136</sup> In the case of drug delivery, loading is primarily restricted to the PFCp shell area since drugs have limited solubility in the

hydrophobic and lipophobic PFC.<sup>174</sup> Therefore, drugs are loaded by conjugating them to the outer layer, loading them within the shell, or within an oil encapsulating layer.<sup>174</sup> However, a recent study utilized microfluidic synthesis to create double emulsion PFCp droplets that encapsulated hydrophilic agents in their core (Fig. 5a from Duncanson *et al.*),<sup>45</sup> Continuing to optimize PFCp synthesis and cargo capabilities could lead to more effective particles.

Gases are much simpler cargo because they are highly soluble within PFCs. Consequently, PFCps have been studied as oxygen carriers and blood substitutes for the past several decades.<sup>14,67,150</sup> Solubility of gases within PFCps is governed by Henry's law, which states that the gas's partial pressure will dictate solubility extent within PFCs. Gaseous delivery is beneficial for several TERM applications. A huge obstacle in SC-based angiogenic therapy is low cell survival upon implantation into ischemic tissue.<sup>100</sup> Increasing available oxygen to SCs until blood vessel ingrowth could improve current therapy outcomes. Groups have shown inclusion of oxygenated PFCps in SC-containing scaffolds increased cell viability and enhanced differentiation.<sup>17,43</sup> PFCps can also deliver other gases such as the signaling molecule NO, which can mitigate vascular diseases like atherosclerosis.<sup>165</sup>

Delivery of therapeutics is usually done in conjunction with US or PA/US. PA/US can be used to track particles *in vivo* and cause release of cargo at the desired site. This is especially true for drug and gene delivery.<sup>132</sup> Gaseous delivery usually relies on simple diffusion across the PFCp shell, but if higher release amounts are desired, PA/US techniques can be used.<sup>165</sup> As previously stated, irradiation of PFCps causes phase change from NDs into MBs. The forceful transition can result in stable cavitation. Similarly, application of US to MBs can cause stable or inertial cavitation.<sup>178</sup> Either way, cavitation exerts mechanical stresses on nearby cells and increases permeability of junctions or membranes allowing for increased delivery and uptake, an effect known as sonoporation.<sup>132,165</sup> In one study, DNA containing MBs were able to achieve successful *in vivo* transfection of neural SCs. Prior to being implanted, neural SCs were loaded with MBs so that each cell had about 1–2 MBs adhered to their membrane or within endosomes. The MBs showed an increased lifetime of 5 days compared to circulation lifetimes of only hours for MBs in aqueous media.<sup>172</sup> US was used to induce cavitation of MBs and subsequent delivery of genes in a controlled manner with high specificity.<sup>172</sup> Whether PA or US is used to trigger cargo release, the contrast provided allows for monitoring the location of PFCps and control over therapeutic delivery, a valuable asset in TERM applications.

Several groups have studied the MB-US combination for increasing attachment of injected MSCs to the desired tissue.<sup>94,194,207</sup> Many TERM applications have a low percentage of SC retention and increasing retention would improve therapies. Localized cell delivery can occur by acoustic manipulation, in which cells coated with functionalized MBs are pushed to desired sites by US waves.<sup>94</sup> A more vigorous approach is to use US to induce cavitation of injected MBs, which causes changes in the microenvironment.<sup>194,207</sup> This method was demonstrated in myocardium infarction models *in vivo*. The targeted cavitation of MBs resulted in increased expression of several cytokines, such as VEGF and vascular cell adhesion molecule 1 (VCAM-1), at the specified site, leading to higher MSC retention and ultimately a better angiogenic response.<sup>207</sup>

Another MIRA application for PFCps is incorporating them into TERM scaffolds. Inclusion of droplet PFCps into scaffolds could control GF delivery.<sup>119</sup> For instance, fibrin hydrogels doped with microdroplets containing basic fibroblast growth factors (bFGF) could be acoustically activated to release bFGF.<sup>48</sup> Release of bFGFs was five times higher with US application. Also, changes in scaffold mechanical properties caused by the transition of droplets into bubbles could be regulated by varying US intensity.<sup>48</sup> These studies were conducted *in vitro*, but show the potential of controlling TERM agent release *in vivo*. This would provide future therapies with control and visualization of therapeutic release and allow treatment customization on a per patient basis.

Apart from inducing mechanical changes in scaffolds, inclusion of PFCps may allow for monitoring scaffold's mechanical properties. Young's moduli of hydrogels can be determined by measuring the displacement of bubbles embedded within the scaffolds.<sup>47,199</sup> This technique has not been studied extensively, but presents an interesting possibility for non-destructive *in vivo* scaffold characterization. Changes in mechanical properties could convey information regarding scaffold degradation or tissue in-growth.

Functionalizing PFCps with targeting ligands benefits therapy delivery and monitoring applications. In therapeutic delivery purposes, it allows for selective treatment of cell types and can be applied with previously addressed therapeutic agents. In monitoring, targeted PFCps can be coupled with either PA/US or <sup>19</sup>F MRI to convey functional and molecular information for assessing therapy progress.<sup>178</sup> For instance, studies that labeled MBs with VEGF receptors were able to track angiogenesis.<sup>143</sup> Although the original purpose was to assess angiogenesis in cancer models, the same technique could be used to monitor TERM revascularization therapies.

Another important parameter to monitor during TERM treatment course is inflammation. *In vivo* studies have shown that injected PFCps are preferentially taken up by circulating monocytes. The labeled cells will migrate towards areas of inflammation and can be detected by <sup>19</sup>F MRI (Fig. 5c from Jacoby *et al.*)<sup>76</sup> Monitoring the extent of inflammation will provide information on TERM treatment effectiveness. Furthermore, therapeutics to reduce inflammation could be loaded within PFCps and enhance their MIRA potential.

### Current Limitations

In terms of clinical feasibility, PFCps have less hurdles to traverse than other agents since certain PFCps, namely MBs, have been FDA approved for several years. However, unlike other MIRAS, PFCps are limited by short lifetimes in aqueous solutions. This limits the window for therapeutic delivery, which is disadvantageous in long-term therapies. Fortunately, since many TERM applications involve cell encapsulation, PFCps can be incorporated into scaffolds and have an extended lifetime of several days.<sup>172</sup> Other concerns regarding PFCps include uncertainty of sonoporation effects. Despite being an active research area for the past 15 years, sonoporation's exact mechanisms remain relatively misunderstood.<sup>49</sup> More studies are needed to elucidate appropriate parameters for inducing cavitation to achieve effective therapeutic outcomes while maintaining cell function.

## Outlook

PFCps demonstrate excellent therapeutic delivery and monitoring capabilities. The fact that several different PFCp contrast agents are FDA approved and have been in clinical use for several years has positive implications for other PFCp applications. PFCps used for targeted delivery are best used in conjunction with US/PA imaging techniques since release can be controlled *via* acoustic or light irradiation. Additionally, supplementing PA to US imaging allows for increased sensitivity and detection. Focus on prolonging the stability of PFCps and using them for longitudinal monitoring applications, such as cell tracking or scaffold assessment would benefit TERM applications. Future areas of interest regarding PFCp use as MIRAs include scaffold assessment in conjunction with shear imaging techniques and monitoring inflammation using  $^{19}\text{F}$  MRI.

## CONCLUSION

MIRAs' combined ability to enhance therapies and monitor different processes present unique opportunities for improving TERM treatments. The reviewed particles all show great potential as therapeutic and imaging agents. However, thus far therapy and imaging are still largely separated, and more research combining these applications is needed. While similar ideas have taken off in other biomedical fields, research related to combined TERM monitoring and therapy is still in its emerging stages. Continuing to study and develop MIRAs could prove critical to clinical translation of TERM therapies by elucidating current knowledge regarding TERM treatments and highlighting areas for improvement. In addition, MIRAs can allow clinicians to noninvasively evaluate treatments *in vivo* and modify therapy immediately. As noted throughout the review, each of the described particles has certain limitations and is often best suited for a specific type of application and imaging modality. Continuing to research MIRAs will give a clearer picture of which agent is best suited for particular TERM therapies. Researchers should also keep in mind hurdles for the described agents gaining FDA approval and strive to demonstrate particle safety through appropriate assays. Given the current state of research for TERM therapy and monitoring and the success of the closely related theranostic particles, there is great potential for MIRAs.

## ABBREVIATIONS

|             |                                 |
|-------------|---------------------------------|
| <b>ADV</b>  | Acoustic droplet vaporization   |
| <b>ALP</b>  | Alkaline phosphatase            |
| <b>AuNC</b> | Gold nanocage                   |
| <b>AuNP</b> | Gold nanoparticle               |
| <b>AuNR</b> | Gold nanorod                    |
| <b>AuNS</b> | Gold nanosphere                 |
| <b>BBB</b>  | Blood-brain barrier             |
| <b>bFGF</b> | Basic fibroblast growth factors |

|              |   |
|--------------|---|
| <b>CNTs</b>  | Carbon nanotubes                                  |
| <b>CT</b>    | Computed tomography                               |
| <b>CTAB</b>  | Cetyltrimethylammonium bromide                    |
| <b>GF</b>    | Growth factor                                     |
| <b>GNB</b>   | Gold nanobeacon                                   |
| <b>HACC</b>  | Hydroxypropyltrimethyl ammonium chloride chitosan |
| <b>HEMA</b>  | (Hydroxyethyl)methacrylate                        |
| <b>ICG</b>   | Indocyanine green                                 |
| <b>IONPs</b> | Iron oxide nanoparticles                          |
| <b>MB</b>    | Microbubble                                       |
| <b>MIRAs</b> | Monitoring/Imaging and Regenerative Agents        |
| <b>MRI</b>   | Magnetic resonance imaging                        |
| <b>MSC</b>   | Mesenchymal stem cell                             |
| <b>MSN</b>   | Mesoporous silica nanoparticle                    |
| <b>MWCNT</b> | Multiple-wall carbon nanotube                     |
| <b>ND</b>    | Nanodroplet                                       |
| <b>NIR</b>   | Near infrared                                     |
| <b>NO</b>    | Nitric oxide                                      |
| <b>PA</b>    | Photoacoustic                                     |
| <b>pDNA</b>  | Plasmid DNA                                       |
| <b>PEG</b>   | Polyethylene glycol                               |
| <b>PEI</b>   | Poly(ethyleneimine)                               |
| <b>PET</b>   | Positron emission tomography                      |
| <b>PFC</b>   | Perfluorocarbon                                   |
| <b>PFCp</b>  | Perfluorocarbon particle                          |
| <b>PLGA</b>  | Poly(lactide-co-glycolide)                        |
| <b>PVA</b>   | Polyvinyl alcohol                                 |
| <b>SC</b>    | Stem cell   |
| <b>SiNP</b>  | Solid silica nanoparticle                         |

|               |  |
|---------------|--|
| <b>SPIONs</b> | Superparamagnetic iron oxide nanoparticles   |
| <b>SPR</b>    | Surface plasmon resonance                    |
| <b>SWCNT</b>  | Single-walled carbon nanotube                |
| <b>TERM</b>   | Tissue engineering and regenerative medicine |
| <b>US</b>     | Ultrasound                                   |
| <b>VCAM-1</b> | Vascular cell adhesion molecule 1            |
| <b>VEGF</b>   | Vascular endothelial growth factor           |
| <b>VEGFR</b>  | Vascular endothelial growth factor receptor  |

## References

1. Alkilany AM, Nalaria PK, Hexel CR, Shaw TJ, Murphy CJ, Wyatt MD. Cellular uptake and cytotoxicity of gold nanorods: Molecular origin of cytotoxicity and surface effects. *Small*. 2009; 5:701–708. [PubMed: 19226599]
2. Ananta JS, Matson ML, Tang AM, Mandal T, Lin S, Wong K, Wong ST, Wilson LJ. Single-walled carbon nanotube materials as  $T_2$ -weighted mri contrast agents. *J Phys Chem C*. 2009; 113:19369–19372.
3. Andreas K, Georgieva R, Ladwig M, Mueller S, Notter M, Sittinger M, Ringe J. Highly efficient magnetic stem cell labeling with citrate-coated superparamagnetic iron oxide nanoparticles for MRI tracking. *Biomaterials*. 2012; 33:4515–4525. [PubMed: 22445482]
4. Anwer K, Kao G, Proctor B, Anscombe I, Florack V, Earls R, Wilson E, McCreery T, Unger E, Rolland A. Ultrasound enhancement of cationic lipid-mediated gene transfer to primary tumors following systemic administration. *Gene Ther*. 2000; 7:1833–1839. [PubMed: 11110415]
5. Appel AA, Anastasio MA, Larson JC, Brey EM. Imaging challenges in biomaterials and tissue engineering. *Biomaterials*. 2013; 34:6615–6630. [PubMed: 23768903]
6. Arriagada FJ, Osseo-Asare K. Phase and dispersion stability effects in the synthesis of silica nanoparticles in a non-ionic reverse microemulsion. *Colloids Surf*. 1992; 69:105–115.
7. Astolfo A, Arfelli F, Schülte E, James S, Mancini L, Menk RH. A detailed study of gold-nanoparticle loaded cells using X-ray based techniques for cell-tracking applications with single-cell sensitivity. *Nanoscale*. 2013; 5:3337–3345. [PubMed: 23467621]
8. Astolfo A, Schülte E, Menk RH, Kirch RD, Juurlink BHJ, Hall C, Harsan LA, Stebel M, Barbetta D, Tromba G, Arfelli F. *In vivo* visualization of gold-loaded cells in mice using X-ray computed tomography. *Nanomed Nanotechnol Biol Med*. 2013; 9:284–292.
9. Bae KH, Kim YB, Lee Y, Hwang J, Park H, Park TG. Bioinspired synthesis and characterization of gadolinium-labeled magnetite nanoparticles for dual contrast T1-and T2-weighted magnetic resonance imaging. *Bioconjug Chem*. 2010; 21:505–512. [PubMed: 20166678]
10. Bakhru SH, Altiok E, Highley C, Delubac D, Suhan J, Hitchens TK, Ho C, Zappe S. Enhanced cellular uptake and long-term retention of chitosan-modified iron-oxide nanoparticles for MRI-based cell tracking. *Int J Nanomed*. 2012; 7:4613.
11. Balakumaran A, Pawelczyk E, Ren J, Sworder B, Chaudhry A, Sabatino M, Stroncek D, Frank JA, Robey PG. Superparamagnetic iron oxide nanoparticles labeling of bone marrow stromal (mesenchymal) cells does not affect their “stemness”. *PLoS ONE*. 2010; 5:e11462. [PubMed: 20628641]
12. Barone PW, Parker RS, Strano MS. *In vivo* fluorescence detection of glucose using a single-walled carbon nanotube optical sensor: design, fluorophore properties, advantages, and disadvantages. *Anal Chem*. 2005; 77:7556–7562. [PubMed: 16316162]

13. Bartczak D, Muskens OL, Sanchez-Elsner T, Kanaras AG, Millar TM. Manipulation of *in vitro* angiogenesis using peptide-coated gold nanoparticles. *ACS Nano*. 2013; 7:5628–5636. [PubMed: 23713973]
14. Bauer J, Zähres M, Zellermann A, Kirsch M, Petrat F, de Groot H, Mayer C. Perfluorocarbon-filled poly (lactide-*co*-glycolide) nano- and microcapsules as artificial oxygen carriers for blood substitutes: a physico-chemical assessment. *J Microencapsul*. 2010; 27:122–132. [PubMed: 20121485]
15. Beck GR Jr, Ha SW, Camalier CE, Yamaguchi M, Li Y, Lee JK, Weitzmann MN. Bioactive silica-based nanoparticles stimulate bone-forming osteoblasts, suppress bone-resorbing osteoclasts, and enhance bone mineral density *in vivo*. *Nanomedicine*. 2012; 8:793–803. [PubMed: 22100753]
16. Beck JS, Vartuli JC, Roth WJ, Leonowicz ME, Kresge CT, Schmitt KD, Chu CTW, Olson DH, Sheppard EW. A new family of mesoporous molecular sieves prepared with liquid crystal templates. *J Am Chem Soc*. 1992; 114:10834–10843.
17. Benjamin S, Sheyn D, Ben-David S, Oh A, Kallai I, Li N, Gazit D, Gazit Z. Oxygenated environment enhances both stem cell survival and osteogenic differentiation. *Tissue Eng Part A*. 2013; 19:748–758. [PubMed: 23215901]
18. Berthiaume F, Maguire TJ, Yarmush ML. Tissue engineering and regenerative medicine: history, progress, and challenges. *Annu Rev Chem Biomol Eng*. 2011; 2:403–430. [PubMed: 22432625]
19. Bock N, Riminucci A, Dionigi C, Russo A, Tampieri A, Landi E, Goranov VA, Marcacci M, Dediu V. A novel route in bone tissue engineering: magnetic biomimetic scaffolds. *Acta Biomater*. 2010; 6:786–796. [PubMed: 19788946]
20. Bonoiu AC, Mahajan SD, Ding H, Roy I, Yong KT, Kumar R, Hu R, Bergey EJ, Schwartz SA, Prasad PN. Nanotechnology approach for drug addiction therapy: gene silencing using delivery of gold nanorod-siRNA nanoplex in dopaminergic neurons. *Proc Natl Acad Sci*. 2009; 106:5546–5550. [PubMed: 19307583]
21. Bulte JW, Kraitchman DL. Iron oxide MR contrast agents for molecular and cellular imaging. *NMR Biomed*. 2004; 17:484–499. [PubMed: 15526347]
22. Cai X, Paratala BS, Hu S, Sitharaman B, Wang LV. Multiscale photoacoustic microscopy of single-walled carbon nanotube-incorporated tissue engineering scaffolds. *Tissue Eng Part C Methods*. 2011; 18:310–317. [PubMed: 22082018]
23. Cai X, Zhang Y, Li L, Choi SW, MacEwan MR, Yao J, Kim C, Xia Y, Wang LV. Investigation of neovascularization in three-dimensional porous scaffolds *in vivo* by a combination of multiscale photoacoustic microscopy and optical coherence tomography. *Tissue Eng Part C Methods*. 2012; 19:120907062030005–120907062030005.
24. Cai X, Hu S, Paratala B, Sitharaman B, Wang LV. Dual-mode photoacoustic microscopy of carbon nanotube incorporated scaffolds in blood and biological tissues. *SPIE BiOS International Society for Optics and Photonics*. 2011:789921–78996.
25. Cao B, Qiu P, Mao C. Mesoporous iron oxide nanoparticles prepared by polyacrylic acid etching and their application in gene delivery to mesenchymal stem cells. *Microsc Res Tech*. 2013; 76:936–941. [PubMed: 23913581]
26. Carena E, Barceló V, Morancho A, Levander L, Boada C, Laromaine A, Roig A, Montaner J, Rosell A. *In vitro* angiogenic performance and *in vivo* brain targeting of magnetized endothelial progenitor cells for neurorepair therapies. *Nanomed Nanotechnol Biol Med*. 2014; 10:225–234.
27. Chan MH, Lin HM. Preparation and identification of multifunctional mesoporous silica nanoparticles for *in vitro* and *in vivo* dual-mode imaging, theranostics, and targeted tracking. *Biomaterials*. 2015; 46:149–158. [PubMed: 25678124]
28. Chen Y, Ai K, Liu J, Sun G, Yin Q, Lu L. Multifunctional envelope-type mesoporous silica nanoparticles for pH-responsive drug delivery and magnetic resonance imaging. *Biomaterials*. 2015; 60:111–120. [PubMed: 25988726]
29. Chen YS, Frey W, Kim S, Homan K, Kruizinga P, Sokolov K, Emelianov S. Enhanced thermal stability of silica-coated gold nanorods for photoacoustic imaging and image-guided therapy. *Opt Express*. 2010; 18:8867–8878. [PubMed: 20588732]

30. Chithrani BD, Chan WCW. Elucidating the mechanism of cellular uptake and removal of protein-coated gold nanoparticles of different sizes and shapes. *Nano Lett.* 2007; 7:1542–1550. [PubMed: 17465586]
31. Choi HS, Liu W, Misra P, Tanaka E, Zimmer JP, Itty Ipe B, Bawendi MG, Frangioni JV. Renal clearance of quantum dots. *Nat Biotechnol.* 2007; 25:1165–1170. [PubMed: 17891134]
32. Chung E, Nam SY, Ricles LM, Emelianov SY, Suggs LJ. Evaluation of gold nanotracers to track adipose-derived stem cells in a PEGylated fibrin gel for dermal tissue engineering applications. *Int J Nanomed.* 2013; 8:325–336.
33. Chung TH, Wu SH, Yao M, Lu CW, Lin YS, Hung Y, Mou CY, Chen YC, Huang DM. The effect of surface charge on the uptake and biological function of mesoporous silica nanoparticles in 3T3-L1 cells and human mesenchymal stem cells. *Biomaterials.* 2007; 28:2959–2966. [PubMed: 17397919]
34. Cirillo G, Hampel S, Spizzirri UG, Parisi OI, Picci N, Iemma F. Carbon nanotubes hybrid hydrogels in drug delivery: a perspective review. *BioMed Res Int.* 2014; 2014:825017. [PubMed: 24587993]
35. Cohen-karni T, Jeong KJ, Tsui JH, Reznor G, Mustata M, Wanunu M, Graham A, Marks C, Bell DC, Langer R, Kohane DS. Nanocomposite gold-silk nano fibers. *Nano Lett.* 2012; 12:10–13.
36. Cook JR, Frey W, Emelianov S. Quantitative photoacoustic imaging of nanoparticles in cells and tissues. *ACS Nano.* 2013; 7:1272–1280. [PubMed: 23312348]
37. Çukur T, Yamada M, Overall WR, Yang P, Nishimura DG. Positive contrast with alternating repetition time SSFP (PARTS): a fast imaging technique for SPIO-labeled cells. *Magn Reson Med.* 2010; 63:427–437. [PubMed: 20099331]
38. Daniel MC, Astruc D. Gold nanoparticles: assembly, supramolecular chemistry, quantum-size-related properties, and applications toward biology, catalysis, and nanotechnology. *Chem Rev.* 2004; 104:293–346. [PubMed: 14719978]
39. De La Zerd A, Zavaleta C, Keren S, Vaithilingam S, Bodapati S, Liu Z, Levi J, Smith BR, Ma TJ, Oralkan O. Carbon nanotubes as photoacoustic molecular imaging agents in living mice. *Nat Nanotechnol.* 2008; 3:557–562. [PubMed: 18772918]
40. de Rosales RTM, Tavaré R, Glaria A, Varma G, Protti A, Blower PJ. 99mTc-bisphosphonate-iron oxide nanoparticle conjugates for dual-modality biomedical imaging. *Bioconjug Chem.* 2011; 22:455–465. [PubMed: 21338098]
41. Delogu LG, Vidili G, Venturelli E, Ménard-Moyon C, Zoroddu MA, Pilo G, Nicolussi P, Ligios C, Bedognetti D, Sgarrella F. Functionalized multiwalled carbon nanotubes as ultrasound contrast agents. *Proc Natl Acad Sci.* 2012; 109:16612–16617. [PubMed: 23012426]
42. Dobson J. Gene therapy progress and prospects: magnetic nanoparticle-based gene delivery. *Gene Ther.* 2006; 13:283–287. [PubMed: 16462855]
43. Douglas TE, Pilarek M, Kalaszczy ska I, Senderek I, Skwarczy ska A, Cuijpers VM, Modrzejewska Z, Lewandowska-Szumiel M, Dubrue P. Enrichment of chitosan hydrogels with perfluorodecalin promotes gelation and stem cell vitality. *Mater Lett.* 2014; 128:79–84.
44. Dumortier H, Lacotte S, Pastorin G, Marega R, Wu W, Bonifazi D, Briand JP, Prato M, Muller S, Bianco A. Functionalized carbon nanotubes are non-cytotoxic and preserve the functionality of primary immune cells. *Nano Lett.* 2006; 6:1522–1528. [PubMed: 16834443]
45. Duncanson WJ, Arriaga LR, Ung WL, Kopechek JA, Porter TM, Weitz DA. Microfluidic fabrication of perfluorohexane-shelled double emulsions for controlled loading and acoustic-triggered release of hydrophilic agents. *Langmuir.* 2014; 30:13765–13770. [PubMed: 25340527]
46. Dvir T, Timko BP, Brigham MD, Naik SR, Karajanagi SS, Levy O, Jin H, Parker KK, Langer R, Kohane DS. Nanowired three-dimensional cardiac patches. *Nat Nanotechnol.* 2011; 6:720–725. [PubMed: 21946708]
47. Erpelding TN, Hollman KW, O'Donnell M. Bubble-based acoustic radiation force elasticity imaging. *IEEE Trans Ultrason Ferroelectr Freq Control.* 2005; 52:971–979. [PubMed: 16118978]
48. Fabiilli ML, Wilson CG, Padilla F, Martín-Saavedra FM, Fowlkes JB, Franceschi RT. Acoustic droplet-hydrogel composites for spatial and temporal control of growth factor delivery and scaffold stiffness. *Acta Biomater.* 2013; 9:7399–7409. [PubMed: 23535233]

49. Fan Z, Kumon RE, Deng CX. Mechanisms of microbubble-facilitated sonoporation for drug and gene delivery. *Ther Deliv*. 2014; 5:467. [PubMed: 24856171]
50. Fan D, Yin Z, Cheong R, Zhu FQ, Cammarata RC, Chien CL, Levchenko A. Subcellular-resolution delivery of a cytokine through precisely manipulated nanowires. *Nat Nanotechnol*. 2010; 5:545–551. [PubMed: 20543835]
51. Farini A, Villa C, Manescu A, Fiori F, Giuliani A, Razini P, Sitzia C, Del Fraro G, Belicchi M, Meregalli M. Novel insight into stem cell trafficking in dystrophic muscles. *Int J Nanomed*. 2012; 7:3059.
52. Ganesh N, Jayakumar R, Koyakutty M, Mony U, Nair SV. Embedded silica nanoparticles in poly(caprolactone) nanofibrous scaffolds enhanced osteogenic potential for bone tissue engineering. *Tissue Eng Part A*. 2012; 18:1867–1881. [PubMed: 22725098]
53. Garcia-Bennett AE, Kozhevnikova M, Konig N, Zhou C, Leao R, Knopfel T, Pankratova S, Trolle C, Berezin V, Bock E, Aldskogius H, Kozlova EN. Delivery of differentiation factors by mesoporous silica particles assists advanced differentiation of transplanted murine embryonic stem cells. *Stem Cells Transl Med*. 2013; 2:906–915. [PubMed: 24089415]
54. Ghafar-Zadeh E, Waldeisen JR, Lee LP. Engineered approaches to the stem cell microenvironment for cardiac tissue regeneration. *Lab Chip*. 2011; 11:3031–3048. [PubMed: 21785806]
55. Ghiazza, M.; Vietti, G. Health and Environmental Safety of Nanomaterials. Torino: University of Torino; 2014. Carbon nanotubes: properties, applications and toxicity.
56. Gong H, Peng R, Liu Z. Carbon nanotubes for biomedical imaging: the recent advances. *Adv Drug Deliv Rev*. 2013; 65:1951–1963. [PubMed: 24184130]
57. Grapentin C, Mayenfels F, Barnert S, Süß R, Schubert R, Temme S, Jacoby C, Schrader J, Flögel U. Optimization of perfluorocarbon nanoemulsions for molecular imaging by 19F MRI.
58. Green DE, Longtin JP, Sitharaman B. The effect of nanoparticle-enhanced photoacoustic stimulation on multipotent marrow stromal cells. *ACS Nano*. 2009; 3:2065–2072. [PubMed: 19606849]
59. Guilak F, Cohen DM, Estes BT, Gimble JM, Liedtke W, Chen CS. Control of stem cell fate by physical interactions with the extracellular matrix. *Cell Stem Cell*. 2009; 5:17–26. [PubMed: 19570510]
60. Gupta AK, Gupta M. Synthesis and surface engineering of iron oxide nanoparticles for biomedical applications. *Biomaterials*. 2005; 26:3995–4021. [PubMed: 15626447]
61. Ha SW, Weitzmann MN, Beck GR. Bioactive silica nanoparticles promote osteoblast differentiation through stimulation of autophagy and direct association with LC3 and p62. *ACS Nano*. 2014; 8:5898–5910. [PubMed: 24806912]
62. Hainfeld JF, Slatkin DN, Focella TM, Smilowitz HM. Gold nanoparticles: a new X-ray contrast agent. *Br J Radiol*. 2006; 79:248–253. [PubMed: 16498039]
63. Hannah A, Luke G, Wilson K, Homan K, Emelianov S. Indocyanine green-loaded photoacoustic nanodroplets: dual contrast nanoconstructs for enhanced photoacoustic and ultrasound imaging. *ACS Nano*. 2013; 8:250–259. [PubMed: 24303934]
64. Hannah AS, VanderLaan D, Chen YS, Emelianov SY. Photoacoustic and ultrasound imaging using dual contrast perfluorocarbon nanodroplets triggered by laser pulses at 1064 nm. *Biomed Opt Express*. 2014; 5:3042–3052. [PubMed: 25401018]
65. Harrison BS, Atala A. Carbon nanotube applications for tissue engineering. *Biomaterials*. 2007; 28:344–353. [PubMed: 16934866]
66. Hartono SB, Phuoc NT, Yu M, Jia Z, Monteiro MJ, Qiao S, Yu C. Functionalized large pore mesoporous silica nanoparticles for gene delivery featuring controlled release and co-delivery. *J Mater Chem B*. 2014; 2:718–726.
67. Henkel-Hanke T. Artificial oxygen carriers: a current review. *AANA J*. 2007; 75:205. [PubMed: 17591302]
68. Himes N, Min JY, Lee R, Brown C, Shea J, Huang X, Xiao YF, Morgan JP, Burstein D, Oettgen P. *In vivo* MRI of embryonic stem cells in a mouse model of myocardial infarction. *Magn Reson Med*. 2004; 52:1214–1219. [PubMed: 15508153]
69. Hirsch A. Functionalization of single-walled carbon nanotubes. *Angew Chem Int Ed*. 2002; 41:1853–1859.

70. Hoare T, Timko BP, Santamaria J, Goya GF, Irusta S, Lau S, Stefanescu CF, Lin D, Langer R, Kohane DS. Magnetically triggered nanocomposite membranes: a versatile platform for triggered drug release. *Nano Lett.* 2011; 11:1395–1400. [PubMed: 21344911]
71. Hong G, Lee JC, Robinson JT, Raaz U, Xie L, Huang NF, Cooke JP, Dai H. Multifunctional *in vivo* vascular imaging using near-infrared II fluorescence. *Nat Med.* 2012; 18:1841–1846. [PubMed: 23160236]
72. Huang X, Zhang F, Wang H, Niu G, Choi KY, Swierczewska M, Zhang G, Gao H, Wang Z, Zhu L, Choi HS, Lee S, Chen X. Mesenchymal stem cell-based cell engineering with multifunctional mesoporous silica nanoparticles for tumor delivery. *Biomaterials.* 2013; 34:1772–1780. [PubMed: 23228423]
73. Huber DL. Synthesis, properties, and applications of iron nanoparticles. *Small.* 2005; 1:482–501. [PubMed: 17193474]
74. Iijima S. Helical microtubules of graphitic carbon. *Nature.* 1991; 354:56–58.
75. Jackson PA, Rahman WNW, Wong CJ, Ackerly T, Geso M. Potential dependent superiority of gold nanoparticles in comparison to iodinated contrast agents. *Eur J Radiol.* 2010; 75:104–109. [PubMed: 19406594]
76. Jacoby C, Temme S, Mayenfels F, Benoit N, Krafft MP, Schubert R, Schrader J, Flögel U. Probing different perfluorocarbons for *in vivo* inflammation imaging by 19F MRI: image reconstruction, biological half-lives and sensitivity. *NMR Biomed.* 2014; 27:261–271. [PubMed: 24353148]
77. Jiang S, Eltoukhy AA, Love KT, Langer R, Anderson DG. Lipidoid-coated iron oxide nanoparticles for efficient DNA and siRNA delivery. *Nano Lett.* 2013; 13:1059–1064. [PubMed: 23394319]
78. Jin Y, Jia C, Huang SW, O'Donnell M, Gao X. Multifunctional nanoparticles as coupled contrast agents. *Nat Commun.* 2010; 1:41. [PubMed: 20975706]
79. Jin Q, Wang Z, Yan F, Deng Z, Ni F, Wu J, Shandas R, Liu X, Zheng H. A novel cationic microbubble coated with stearic acid-modified polyethylenimine to enhance DNA loading and gene delivery by ultrasound. *PLoS ONE.* 2013; 8:e76544. [PubMed: 24086748]
80. Jing XH, Yang L, Duan XJ, Xie B, Chen W, Li Z, Tan HB. *In vivo* MR imaging tracking of magnetic iron oxide nanoparticle labeled, engineered, autologous bone marrow mesenchymal stem cells following intra-articular injection. *Joint Bone Spine.* 2008; 75:432–438. [PubMed: 18448377]
81. John R, Boppart SA. Magnetomotive molecular nanoprobe. *Curr Med Chem.* 2011; 18:2103. [PubMed: 21517766]
82. Jokerst JV, Khademi C, Gambhir SS. Intracellular aggregation of multimodal silica nanoparticles for ultrasound-guided stem cell implantation. *Sci Transl Med.* 2013; 5:177ra135.
83. Jokerst JV, Thangaraj M, Kempen PJ, Sinclair R, Gambhir SS. Photoacoustic imaging of mesenchymal stem cells in living mice via silica-coated gold nanorods. *ACS Nano.* 2012; 6:5920–5930. [PubMed: 22681633]
84. José-Yacamán M, Miki-Yoshida M, Rendon L, Santiesteban J. Catalytic growth of carbon microtubules with fullerene structure. *Appl Phys Lett.* 1993; 62:202–204.
85. Jung CW, Jacobs P. Physical and chemical properties of superparamagnetic iron oxide MR contrast agents: ferumoxides, ferumoxtran, ferumoxsil. *Magn Reson Imaging.* 1995; 13:661–674. [PubMed: 8569441]
86. Kam NWS, O'Connell M, Wisdom JA, Dai H. Carbon nanotubes as multifunctional biological transporters and near-infrared agents for selective cancer cell destruction. *Proc Natl Acad Sci USA.* 2005; 102:11600–11605. [PubMed: 16087878]
87. Kemp MM, Kumar A, Mousa S, Dyskin E, Yalcin M, Ajayan P, Linhardt RJ, Mousa SA. Gold and silver nanoparticles conjugated with heparin derivative possess anti-angiogenesis properties. *Nanotechnology.* 2009; 20:455104. [PubMed: 19822927]
88. Kempen PJ, Greasley S, Parker KA, Campbell JL, Chang HY, Jones JR, Sinclair R, Gambhir SS, Jokerst JV. Theranostic mesoporous silica nanoparticles biodegrade after pro-survival drug delivery and ultrasound/magnetic resonance imaging of stem cells. *Theranostics.* 2015; 5:631–642. [PubMed: 25825602]

89. Khandare JJ, Jalota-Badhwar A, Satavalekar SD, Bhansali SG, Aher ND, Kharas F, Banerjee SS. PEG-conjugated highly dispersive multifunctional magnetic multi-walled carbon nanotubes for cellular imaging. *Nanoscale*. 2012; 4:837–844. [PubMed: 22170574]
90. Kievit FM, Veiseh O, Bhattarai N, Fang C, Gunn JW, Lee D, Ellenbogen RG, Olson JM, Zhang M. PEI-PEG-chitosan-copolymer-coated iron oxide nanoparticles for safe gene delivery: synthesis, complexation, and transfection. *Adv Funct Mater*. 2009; 19:2244–2251. [PubMed: 20160995]
91. Kim JW, Galanzha EI, Shashkov EV, Moon HM, Zharov VP. Golden carbon nanotubes as multimodal photoacoustic and photothermal high-contrast molecular agents. *Nat Nanotechnol*. 2009; 4:688–694. [PubMed: 19809462]
92. Kim JH, Kim MH, Jo DH, Yu YS, Lee TG, Kim JH. The inhibition of retinal neovascularization by gold nanoparticles via suppression of VEGFR-2 activation. *Biomaterials*. 2011; 32:1865–1871. [PubMed: 21145587]
93. Klibanov AL. Ligand-carrying gas-filled microbubbles: ultrasound contrast agents for targeted molecular imaging. *Bioconjug Chem*. 2005; 16:9–17. [PubMed: 15656569]
94. Kokhuis T, Skachkov I, Naaijken B, Juffermans L, Kamp O, van der Steen A, Versluis M, de Jong N. StemBells: localized stem cell delivery using targeted microbubbles and acoustic radiation force. *J Acoust Soc Am*. 2014; 135:2310–2310.
95. Kong L, Alves CS, Hou W, Qiu J, Möhwald H, Tomás H, Shi X. RGD Peptide-Modified Dendrimer-Entrapped Gold Nanoparticles Enable Highly Efficient and Specific Gene Delivery to Stem Cells. *ACS Appl Mater Interfaces*. 2015; 7:4833–4843. [PubMed: 25658033]
96. Korzeniowska B, Nooney R, Wencel D, McDonagh C. Silica nanoparticles for cell imaging and intracellular sensing. *Nanotechnology*. 2013; 24:442002. [PubMed: 24113689]
97. Kresge CT, Leonowicz ME, Roth WJ, Vartuli JC, Beck JS. Ordered mesoporous molecular sieves synthesized by a liquid-crystal template mechanism. *Nature*. 1992; 359:710–712.
98. Lalwani G, Gopalan A, D'Agati M, Srinivas Sankaran J, Judex S, Qin YX, Sitharaman B. Porous three-dimensional carbon nanotube scaffolds for tissue engineering. *J Biomed Mater Res Part A*. 2015; 103:3212–3225.
99. Laurent S, Forge D, Port M, Roch A, Robic C, Vander Elst L, Muller RN. Magnetic iron oxide nanoparticles: synthesis, stabilization, vectorization, physicochemical characterizations, and biological applications. *Chem Rev*. 2008; 108:2064–2110. [PubMed: 18543879]
100. Lee HY, Kim HW, Lee JH, Oh SH. Controlling oxygen release from hollow microparticles for prolonged cell survival under hypoxic environment. *Biomaterials*. 2015; 53:583–591. [PubMed: 25890754]
101. Lee JH, Lee JY, Yang SH, Lee EJ, Kim HW. Carbon nanotube–collagen three-dimensional culture of mesenchymal stem cells promotes expression of neural phenotypes and secretion of neurotrophic factors. *Acta Biomater*. 2014; 10:4425–4436. [PubMed: 24954912]
102. Lee HY, Li Z, Chen K, Hsu AR, Xu C, Xie J, Sun S, Chen X. PET/MRI dual-modality tumor imaging using arginine-glycine-aspartic (RGD)-conjugated radiolabeled iron oxide nanoparticles. *J Nucl Med*. 2008; 49:1371–1379. [PubMed: 18632815]
103. Leu JG, Chen SA, Chen HM, Wu WM, Hung CF, Yao YD, Tu CS, Liang YJ. The effects of gold nanoparticles in wound healing with antioxidant epigallocatechin gallate and  $\alpha$ -lipoic acid. *Nanomed Nanotechnol Biol Med*. 2012; 8:767–775.
104. Levy I, Sher I, Corem-Salkmon E, Ziv-Polat O, Meir A, Treves AJ, Nagler A, Kalter-Leibovici O, Margel S, Rotenstreich Y. Bioactive magnetic near Infra-Red fluorescent core-shell iron oxide/human serum albumin nanoparticles for controlled release of growth factors for augmentation of human mesenchymal stem cell growth and differentiation. *J Nanobiotechnol*. 2015; 13:1–14.
105. Lewandowska-Łaucka J, Fiejdasz S, Rodzik Ł, Kozieł M, Nowakowska M. Bioactive hydrogel-nanosilica hybrid materials: a potential injectable scaffold for bone tissue engineering. *Biomed Mater*. 2015; 10:015020. [PubMed: 25668107]
106. Li Y, Huang G, Zhang X, Li B, Chen Y, Lu T, Lu TJ, Xu F. Magnetic hydrogels and their potential biomedical applications. *Adv Funct Mater*. 2013; 23:660–672.
107. Li X, Liu H, Niu X, Yu B, Fan Y, Feng Q, Cui FZ, Watari F. The use of carbon nanotubes to induce osteogenic differentiation of human adipose-derived MSCs *in vitro* and ectopic bone formation *in vivo*. *Biomaterials*. 2012; 33:4818–4827. [PubMed: 22483242]

108. Liu Z, Davis C, Cai W, He L, Chen X, Dai H. Circulation and long-term fate of functionalized, bio-compatible single-walled carbon nanotubes in mice probed by Raman spectroscopy. *Proc Natl Acad Sci*. 2008; 105:1410–1415. [PubMed: 18230737]
109. Liu G, Hong R, Guo L, Li Y, Li H. Preparation, characterization and MRI application of carboxymethyl dextran coated magnetic nanoparticles. *Appl Surf Sci*. 2011; 257:6711–6717.
110. Liu Z, Li X, Tabakman SM, Jiang K, Fan S, Dai H. Multiplexed multicolor Raman imaging of live cells with isotopically modified single walled carbon nanotubes. *J Am Chem Soc*. 2008; 130:13540–13541. [PubMed: 18803379]
111. Liu D, Yi C, Zhang D, Zhang J, Yang M. Inhibition of proliferation and differentiation of mesenchymal stem cells by carboxylated carbon nanotubes. *ACS Nano*. 2010; 4:2185–2195. [PubMed: 20218664]
112. Ma N, Cheng H, Lu M, Liu Q, Chen X, Yin G, Zhu H, Zhang L, Meng X, Tang Y. Magnetic resonance imaging with superparamagnetic iron oxide fails to track the long-term fate of mesenchymal stem cells transplanted into heart. *Sci Rep*. 2015; 5:9058. [PubMed: 25762186]
113. Mahmoudi M, Simchi A, Imani M, Milani AS, Stroeve P. Optimal design and characterization of super-paramagnetic iron oxide nanoparticles coated with polyvinyl alcohol for targeted delivery and imaging. *J Phys Chem B*. 2008; 112:14470–14481. [PubMed: 18729404]
114. Main ML, Grayburn PA. Clinical applications of transpulmonary contrast echocardiography. *Am Heart J*. 1999; 137:144–153. [PubMed: 9878947]
115. Mehrmohammadi M, Shin TH, Qu M, Kruizinga P, Truby RL, Lee JH, Cheon J, Emelianov SY. *In vivo* pulsed magneto-motive ultrasound imaging using high-performance magnetoactive contrast nanoagents. *Nanoscale*. 2013; 5:11179–11186. [PubMed: 24080913]
116. Menk RH, Schültke E, Hall C, Arfelli F, Astolfo A, Rigon L, Round A, Ataelmannan K, MacDonald SR, Juurlink BHJ. Gold nanoparticle labeling of cells is a sensitive method to investigate cell distribution and migration in animal models of human disease. *Nanomed Nanotechnol Biol Med*. 2011; 7:647–654.
117. Mikael PE, Amini AR, Basu J, Arellano-Jimenez MJ, Laurencin CT, Sanders MM, Carter CB, Nukavarapu SP. Functionalized carbon nanotube reinforced scaffolds for bone regenerative engineering: fabrication, *in vitro* and *in vivo* evaluation. *Biomed Mater*. 2014; 9:035001. [PubMed: 24687391]
118. Mok H, Zhang M. Superparamagnetic iron oxide nanoparticle-based delivery systems for biotherapeutics. *Expert Opin Drug Deliv*. 2013; 10:73–87. [PubMed: 23199200]
119. Moncion A, Kripfgans OD, Carson PL, Fowlkes JB, Fabiilli ML. Characterization of acoustic droplet vaporization and inertial cavitation thresholds in acoustically-responsive tissue scaffolds. *Ultrasonics Symposium*. 2014
120. Moon GD, Choi SW, Cai X, Li W, Cho EC, Jeong U. A new theranostic system based on gold nanocages and phase-change materials with unique features for photoacoustic imaging and controlled release. *JACS*. 2011; 133:4762–4765.
121. Mooney E, Dockery P, Greiser U, Murphy M, Barron V. Carbon nanotubes and mesenchymal stem cells: biocompatibility, proliferation and differentiation. *Nano Lett*. 2008; 8:2137–2143. [PubMed: 18624387]
122. Mooney E, Mackle JN, Blond DJP, O’Cearbhaill E, Shaw G, Blau WJ, Barry FP, Barron V, Murphy JM. The electrical stimulation of carbon nanotubes to provide a cardiomimetic cue to MSCs. *Biomaterials*. 2012; 33:6132–6139. [PubMed: 22681974]
123. Moradian H, Fasehee H, Keshvari H, Faghihi S. Poly (ethyleneimine) functionalized carbon nanotubes as efficient nano-vector for transfecting mesenchymal stem cells. *Colloids Surf B*. 2014; 122:115–125.
124. Mukherjee P, Bhattacharya R, Wang P, Wang L, Basu S, Nagy JA, Atala A, Mukhopadhyay D, Soker S. Antiangiogenic properties of gold nanoparticles. *Clin Cancer Res*. 2005; 11:3530–3534. [PubMed: 15867256]
125. Muroski ME, Morgan TJ, Levenson CW, Strouse F. A gold nanoparticle pentapeptide: gene fusion to induce therapeutic gene expression in mesenchymal stem cells. *J Am Chem Soc*. 2014; 136:14763–14771. [PubMed: 25198921]

126. Nam SY, Ricles LM, Suggs LJ, Emelianov SY. *In vivo* ultrasound and photoacoustic monitoring of mesenchymal stem cells labeled with gold nanotracers. *PLoS ONE*. 2012; 7:1–9.
127. Nam SY, Ricles LM, Suggs LJ, Emelianov SY. Imaging strategies for tissue engineering applications. *Tissue Eng Part B*. 2014; 21:88–102.
128. Ohgushi M, Nagayama K, Wada A. Dextran-magnetite: a new relaxation reagent and its application to T<sub>2</sub> measurements in gel systems. *J Magn Reson*. 1978; 29:599–601.
129. Oldenburg A, Toublan F, Suslick K, Wei A, Boppart S. Magnetomotive contrast for *in vivo* optical coherence tomography. *Opt Express*. 2005; 13:6597–6614. [PubMed: 19498675]
130. Olsson MB, Persson BR, Salford LG, Schröder U. Ferromagnetic particles as contrast agent in T<sub>2</sub> NMR imaging. *Magn Reson Imaging*. 1986; 4:437–440.
131. Orza A, Soritau O, Olenic L, Diudea M, Florea A, Rus Ciuca D, Miha C, Casciano D, Biris AS. Electrically conductive gold-coated collagen nanofibers for placental-derived mesenchymal stem cells enhanced differentiation and proliferation. *ACS Nano*. 2011; 5:4490–4503. [PubMed: 21609025]
132. Otani K, Yamahara K, Ohnishi S, Obata H, Kitamura S, Nagaya N. Nonviral delivery of siRNA into mesenchymal stem cells by a combination of ultrasound and microbubbles. *J Control Release*. 2009; 133:146–153. [PubMed: 18976686]
133. O'connell, MJ. Carbon Nanotubes: Properties and Applications. Boca Raton: CRC Press; 2006.
134. Pan L, He Q, Liu J, Chen Y, Ma M, Zhang L, Shi J. Nuclear-targeted drug delivery of TAT peptide-conjugated monodisperse mesoporous silica nanoparticles. *J Am Chem Soc*. 2012; 134:5722–5725. [PubMed: 22420312]
135. Pan D, Pramanik M, Senpan A, Allen JS, Zhang H, Wickline SA, Wang LV, Lanza GM. Molecular photoacoustic imaging of angiogenesis with integrin-targeted gold nanobeacons. *FASEB J*. 2011; 25:875–882. [PubMed: 21097518]
136. Panje CM, Wang DS, Pysz MA, Paulmurugan R, Ren Y, Tranquart F, Tian L, Willmann JK. Ultrasound-mediated gene delivery with cationic versus neutral microbubbles: effect of DNA and microbubble dose on *in vivo* transfection efficiency. *Theranostics*. 2012; 2:1078. [PubMed: 23227124]
137. Park JW, Ku SH, Moon HH, Lee M, Choi D, Yang J, Huh YM, Jeong JH, Park TG, Mok H. Cross-linked iron oxide nanoparticles for therapeutic engineering and *in vivo* monitoring of mesenchymal stem cells in cerebral ischemia model. *Macromol Biosci*. 2014; 14:380–389. [PubMed: 24634264]
138. Park W, Yang HN, Ling D, Yim H, Kim KS, Hyeon T, Na K, Park KH. Multi-modal transfection agent based on monodisperse magnetic nanoparticles for stem cell gene delivery and tracking. *Biomaterials*. 2014; 35:7239–7247. [PubMed: 24881029]
139. Pastine SJ, Okawa D, Zettl A, Fréchet JM. Chemicals on demand with phototriggerable microcapsules. *J Am Chem Soc*. 2009; 131:13586–13587. [PubMed: 19736938]
140. Patlolla A, Knighten B, Tchounwou P. Multi-walled carbon nanotubes induce cytotoxicity, genotoxicity and apoptosis in normal human dermal fibroblast cells. *Ethn Dis*. 2010; 20:S1. [PubMed: 20521388]
141. Phillips E, Penate-Medina O, Zanzonico PB, Carvajal RD, Mohan P, Ye Y, Humm J, Gönen M, Kalaigian H, Schöder H, Strauss HW, Larson SM, Wiesner U, Bradbury MS. Clinical translation of an ultrasmall inorganic optical-PET imaging nanoparticle probe. *Sci Transl Med*. 2014; 6:260.
142. Plank C, Zelphati O, Mykhaylyk O. Magnetically enhanced nucleic acid delivery. Ten years of magnetofection—Progress and prospects. *Adv Drug Deliv Rev*. 2011; 63:1300–1331. [PubMed: 21893135]
143. Pochon S, Tardy I, Bussat P, Bettinger T, Brochot J, von Wronski M, Passantino L, Schneider M. BR55: a lipopeptide-based VEGFR2-targeted ultrasound contrast agent for molecular imaging of angiogenesis. *Invest Radiol*. 2010; 45:89–95. [PubMed: 20027118]
144. Poologasundarampillai G, Yu B, Tsigkou O, Valliant E, Yue S, Lee PD, Hamilton RW, Stevens MM, Kasuga T, Jones JR. Bioactive silica-poly( $\gamma$ -glutamic acid) hybrids for bone regeneration: effect of covalent coupling on dissolution and mechanical properties and fabrication of porous scaffolds. *Soft Matter*. 2012; 8:4822–4832.

145. Prato M, Kostarelos K, Bianco A. Functionalized carbon nanotubes in drug design and discovery. *Acc Chem Res.* 2007; 41:60–68. [PubMed: 17867649]
146. Richard C, Doan BT, Beloeil JC, Bessodes M, Tóth É, Scherman D. Noncovalent functionalization of carbon nanotubes with amphiphilic Gd<sup>3+</sup> chelates: toward powerful  $T_1$  and  $T_2$  MRI contrast agents. *Nano Lett.* 2008; 8:232–236. [PubMed: 18088153]
147. Ricles LM, Nam SY, Sokolov K, Emelianov SY, Suggs LJ. Function of mesenchymal stem cells following loading of gold nanotracers. *Int J Nanomed.* 2011; 6:407–416.
148. Ricles LM, Nam SY, Treviño EA, Emelianov SY, Suggs LJ. A dual gold nanoparticle system for mesenchymal stem cell tracking. *J Mater Chem B.* 2014; 2:8220–8230.
149. Riegler J, Liew A, Hynes SO, Ortega D, O'Brien T, Day RM, Richards T, Sharif F, Pankhurst QA, Lythgoe MF. Superparamagnetic iron oxide nanoparticle targeting of MSCs in vascular injury. *Biomaterials.* 2013; 34:1987–1994. [PubMed: 23237516]
150. Riess JG. Understanding the fundamentals of perfluorocarbons and perfluorocarbon emulsions relevant to *in vivo* oxygen delivery. *Artif Cells Blood Substit Biotechnol.* 2005; 33:47–63.
151. Ruiz-Cabello J, Barnett BP, Bottomley PA, Bulte JW. Fluorine (19F) MRS and MRI in biomedicine. *NMR Biomed.* 2011; 24:114–129. [PubMed: 20842758]
152. Scapin G, Salice P, Tescari S, Menna E, De Filippis V, Filippini F. Enhanced neuronal cell differentiation combining biomimetic peptides and a carbon nanotube-polymer scaffold. *Nanomed Nanotechnol Biol Med.* 2015; 11:621–632.
153. Schöni DS, Bogni S, Bregy A, Wirth A, Raabe A, Vajtai I, Pielers U, Reinert M, Frenz M. Nanoshell assisted laser soldering of vascular tissue. *Lasers Surg Med.* 2011; 43:975–983. [PubMed: 22109727]
154. Sheeran PS, Luo S, Dayton PA, Matsunaga TO. Formulation and acoustic studies of a new phaseshift agent for diagnostic and therapeutic ultrasound. *Langmuir.* 2011; 27:10412–10420. [PubMed: 21744860]
155. Siefker J, Karande P, Coppens MO. Packaging biological cargoes in mesoporous materials: opportunities for drug delivery. *Expert Opin Drug Deliv.* 2014; 11:1781–1793. [PubMed: 25016923]
156. Singh MK, Gracio J, LeDuc P, Gonçalves PP, Marques PA, Gonçalves G, Marques F, Silva VS, Silva FCE, Reis J. Integrated biomimetic carbon nanotube composites for *in vivo* systems. *Nanoscale.* 2010; 2:2855–2863. [PubMed: 20936241]
157. Siqueira IAB, Corat MA, Cavalcanti BDN, Neto WAR, Martin AA, Bretas RES, Marciano FR, Lobo AO. In vitro and in vivo studies of a novel poly (D, L-lactic acid), superhydrophilic carbon nanotubes and nanohydroxyapatite scaffolds for bone regeneration. *ACS Appl Mater Interfaces.* 2015
158. Skrabalak SE, Chen J, Sun Y, Lu X, Au L, Cogley CM, Xia Y. Gold nanocages: synthesis, properties, and applications. *Acc Chem Res.* 2008; 41:1587–1595. [PubMed: 18570442]
159. Slowing II, Trewyn BG, Lin VSY. Mesoporous silica nanoparticles for intracellular delivery of membrane-impermeable proteins. *J Am Chem Soc.* 2007; 129:8845–8849. [PubMed: 17589996]
160. Slowing II, Vivero-Escoto JL, Trewyn BG, Lin VSY. Mesoporous silica nanoparticles: structural design and applications. *J Mater Chem.* 2010; 20:7924–7937.
161. Stephen ZR, Kievit FM, Zhang M. Magnetite nanoparticles for medical MR imaging. *Mater Today.* 2011; 14:330–338.
162. Stöber W, Fink A, Bohn E. Controlled growth of monodisperse silica spheres in the micron size range. *J Colloid Interface Sci.* 1968; 26:62–69.
163. Suh JS, Lee JY, Choi YS, Yu F, Yang V, Lee SJ, Chung CP, Park YJ. Efficient labeling of mesenchymal stem cells using cell permeable magnetic nanoparticles. *Biochem Biophys Res Commun.* 2009; 379:669–675. [PubMed: 19101509]
164. Sun Z, Yathindranath V, Worden M, Thliveris JA, Chu S, Parkinson FE, Hegmann T, Miller DW. Characterization of cellular uptake and toxicity of aminosilane-coated iron oxide nanoparticles with different charges in central nervous system-relevant cell culture models. *Int J Nanomed.* 2013; 8:961.

165. Sutton J, Raymond J, Verleye M, Pyne-Geithman G, Holland C. Pulsed ultrasound enhances the delivery of nitric oxide from bubble liposomes to ex vivo porcine carotid tissue. *Int J Nanomed.* 2014; 9:4671.
166. Sykova E, Jendelova P. Migration, fate and *in vivo* imaging of adult stem cells in the CNS. *Cell Death Differ.* 2007; 14:1336–1342. [PubMed: 17396130]
167. Talaie T, Pratt SJ, Vanegas C, Xu S, Henn RF, Yarowsky P, Lovering RM. Site-specific targeting of platelet-rich plasma via superparamagnetic nanoparticles. *Orthop J Sports Med.* 2015; 3:2325967114566185.
168. Talukdar Y, Avti P, Sun J, Sitharaman B. Multi-modal ultrasound-photoacoustic imaging of tissue engineering scaffolds and blood oxygen saturation in and around the scaffolds. *Tissue Eng Part C Methods.* 2014; 20:440–449. [PubMed: 24107069]
169. Tan B, Rankin SE. Dual latex/surfactant templating of hollow spherical silica particles with ordered mesoporous shells. *Langmuir.* 2005; 21:8180–8187. [PubMed: 16114920]
170. Tang S, Tang Y, Zhong L, Murat K, Asan G, Yu J, Jian R, Wang C, Zhou P. Short-and long-term toxicities of multi-walled carbon nanotubes *in vivo* and *in vitro*. *J Appl Toxicol.* 2012; 32:900–912. [PubMed: 22760929]
171. Tarn D, Ashley CE, Xue M, Carnes EC, Zink JJ, Brinker CJ. Mesoporous silica nanoparticle nanocarriers: biofunctionality and biocompatibility. *Acc Chem Res.* 2013; 46:792–801. [PubMed: 23387478]
172. Tavri S, Vezeridis A, Cui W, Mattrey RF. *In vivo* transfection and detection of gene expression of stem cells preloaded with DNA-carrying microbubbles. *Radiology.* 2015; 276:518–525. [PubMed: 25811427]
173. Terrovitis J, Stuber M, Youssef A, Preece S, Leppo M, Kizana E, Scha'ar M, Gerstenblith G, Weiss RG, Marbán E. Magnetic resonance imaging overestimates ferumoxide-labeled stem cell survival after transplantation in the heart. *Circulation.* 2008; 117:1555–1562. [PubMed: 18332264]
174. Tinkov S, Bekeredjian R, Winter G, Coester C. Microbubbles as ultrasound triggered drug carriers. *J Pharm Sci.* 2009; 98:1935–1961. [PubMed: 18979536]
175. Tran PA, Zhang L, Webster TJ. Carbon nanofibers and carbon nanotubes in regenerative medicine. *Adv Drug Deliv Rev.* 2009; 61:1097–1114. [PubMed: 19647768]
176. Trewyn BG I, Slowing I, Giri S, Chen HT, Lin VSY. Synthesis and functionalization of a mesoporous silica nanoparticle based on the sol-gel process and applications in controlled release. *Acc Chem Res.* 2007; 40:846–853. [PubMed: 17645305]
177. Ulissi ZW, Sen F, Gong X, Sen S, Iverson N, Boghossian AA, Godoy LC, Wogan GN, Mukhopadhyay D, Strano MS. Spatiotemporal intracellular nitric oxide signaling captured using internalized, near-infrared fluorescent carbon nanotube nanosensors. *Nano Lett.* 2014; 14:4887–4894. [PubMed: 25029087]
178. Unger E, Porter T, Lindner J, Grayburn P. Cardiovascular drug delivery with ultrasound and microbubbles. *Adv Drug Deliv Rev.* 2014; 72:110–126. [PubMed: 24524934]
179. Varner VD, Nelson CM. Toward the directed self-assembly of engineered tissues. *Annu Rev Chem Biomol Eng.* 2014; 5:507–526. [PubMed: 24797818]
180. Vashist SK, Zheng D, Pastorin G, Al-Rubeaan K, Luong JH, Sheu FS. Delivery of drugs and biomolecules using carbon nanotubes. *Carbon.* 2011; 49:4077–4097.
181. Villa C, Erratico S, Razini P, Fiori F, Rustichelli F, Torrente Y, Belicchi M. Stem cell tracking by nanotechnologies. *Int J Mol Sci.* 2010; 11:1070–1081. [PubMed: 20480000]
182. Vittorio O, Duce SL, Pietrabissa A, Cuschieri A. Multiwall carbon nanotubes as MRI contrast agents for tracking stem cells. *Nanotechnology.* 2011; 22:095706. [PubMed: 21270482]
183. Vivero-Escoto JL, Huxford-Phillips RC, Lin W. Silica-based nanoprobe for biomedical imaging and theranostic applications. *Chem Soc Rev.* 2012; 41:2673–2685. [PubMed: 22234515]
184. Wahajuddin SA. Superparamagnetic iron oxide nanoparticles: magnetic nanoplateforms as drug carriers. *Int J Nanomed.* 2012; 7:3445.
185. Wang YXJ, Hussain SM, Krestin GP. Superparamagnetic iron oxide contrast agents: physicochemical characteristics and applications in MR imaging. *Eur Radiol.* 2001; 11:2319–2331. [PubMed: 11702180]

186. Wang C, Ma X, Ye S, Cheng L, Yang K, Guo L, Li C, Li Y, Liu Z. Protamine functionalized single-walled carbon nanotubes for stem cell labeling and *in vivo* Raman/magnetic resonance/photoacoustic triple-modal imaging. *Adv Funct Mater.* 2012; 22:2363–2375.
187. Weissleder RA, Stark D, Engelstad B, Bacon B, Compton C, White D, Jacobs P, Lewis J. Superparamagnetic iron oxide: pharmacokinetics and toxicity. *Am J Roentgenol.* 1989; 152:167–173. [PubMed: 2783272]
188. Wick P, Manser P, Limbach LK, Dettlaff-Weglikowska U, Krumeich F, Roth S, Stark WJ, Bruinink A. The degree and kind of agglomeration affect carbon nanotube cytotoxicity. *Toxicol Lett.* 2007; 168:121–131. [PubMed: 17169512]
189. Widder KJ, Senyei AE, Scarpelli DG. Magnetic microspheres: a model system for site specific drug delivery *in vivo*. *Exp Biol Med.* 1978; 158:141–146.
190. Wilson K, Homan K, Emelianov S. Biomedical photoacoustics beyond thermal expansion using triggered nanodroplet vaporization for contrast-enhanced imaging. *Nat Commun.* 2012; 3:618. [PubMed: 22233628]
191. Wu H, Shi H, Zhang H, Wang X, Yang Y, Yu C, Hao C, Du J, Hu H, Yang S. Prostate stem cell antigen antibody-conjugated multiwalled carbon nanotubes for targeted ultrasound imaging and drug delivery. *Biomaterials.* 2014; 35:5369–5380. [PubMed: 24709520]
192. Xie J, Lee S, Chen X. Nanoparticle-based theranostic agents. *Adv Drug Deliv Rev.* 2010; 62:1064–1079. [PubMed: 20691229]
193. Xie J, Xu C, Kohler N, Hou Y, Sun S. Controlled PEGylation of monodisperse Fe<sub>3</sub>O<sub>4</sub> nanoparticles for reduced non-specific uptake by macrophage cells. *Adv Mater.* 2007; 19:3163–3166.
194. Xu YL, Gao YH, Liu Z, Tan KB, Hua X, Fang ZQ, Wang YL, Wang YJ, Xia HM, Zhuo ZX. Myocardium-targeted transplantation of mesenchymal stem cells by diagnostic ultrasound-mediated microbubble destruction improves cardiac function in myocardial infarction of New Zealand rabbits. *Int J Cardiol.* 2010; 138:182–195. [PubMed: 19383567]
195. Yanagi T, Kajiya H, Kawaguchi M, Kido H, Fukushima T. Photothermal stress triggered by near infrared-irradiated carbon nanotubes promotes bone deposition in rat calvarial defects. *J Biomater Appl.* 2015; 29:1109–1118. [PubMed: 25336291]
196. Yang N, Chen X, Ren T, Zhang P, Yang D. Carbon nanotube based biosensors. *Sens Actuators B Chem.* 2015; 207:690–715.
197. Yang W, Thordarson P, Gooding JJ, Ringer SP, Braet F. Carbon nanotubes for biological and biomedical applications. *Nanotechnology.* 2007; 18:412001.
198. Yi C, Liu D, Fong CC, Zhang J, Yang M. Gold nanoparticles promote osteogenic differentiation of mesenchymal stem cells through p38 MAPK pathway. *ACS Nano.* 2010; 4:6439–6448. [PubMed: 21028783]
199. Yoon S, Aglyamov S, Karpouk A, Emelianov S. A high pulse repetition frequency ultrasound system for the ex vivo measurement of mechanical properties of crystalline lenses with laser-induced microbubbles interrogated by acoustic radiation force. *Phys Med Biol.* 2012; 57:4871. [PubMed: 22797709]
200. Yoon SJ, Mallidi S, Tam JM, Tam JO, Murthy A, Joshi P, Johnston KP, Sokolov KV, Emelianov SY. Biodegradable plasmonic nanoclusters as contrast agent for photoacoustic imaging. *Proceedings of SPIE.* 2010
201. You JO, Rafat M, Ye GJC, Auguste DT. Nanoengineering the heart: conductive scaffolds enhance connexin 43 expression. *Nano Lett.* 2011; 11:3643–3648. [PubMed: 21800912]
202. Zang R, Yang ST. Multiwalled carbon nanotube-coated polyethylene terephthalate fibrous matrices for enhanced neuronal differentiation of mouse embryonic stem cells. *J Mater Chem B.* 2013; 1:646–653.
203. Zerda ADL, Liu Z, Bodapati S, Teed R, Vaithilingam S, Khuri-Yakub BT, Chen X, Dai H, Gambhir SS. Ultrahigh sensitivity carbon nanotube agents for photoacoustic molecular imaging in living mice. *Nano Lett.* 2010; 10:2168–2172. [PubMed: 20499887]
204. Zhang YS, Wang Y, Wang L, Wang Y, Cai X, Zhang C, Wang LV, Xia Y. Labeling human mesenchymal stem cells with gold nanocages for *in vitro* and *in vivo* tracking by two-photon microscopy and photoacoustic microscopy. *Theranostics.* 2013; 3:532–543. [PubMed: 23946820]

205. Zhao X, Kim J, Cezar CA, Huebsch N, Lee K, Bouhadir K, Mooney DJ. Active scaffolds for on-demand drug and cell delivery. *Proc Natl Acad Sci*. 2011; 108:67–72. [PubMed: 21149682]
206. Zhao Q, Langley J, Lee S, Liu W. Positive contrast technique for the detection and quantification of superparamagnetic iron oxide nanoparticles in MRI. *NMR Biomed*. 2011; 24:464–472. [PubMed: 20931569]
207. Zhong S, Shu S, Wang Z, Luo J, Zhong W, Ran H, Zheng Y, Yin Y, Ling Z. Enhanced homing of mesenchymal stem cells to the ischemic myocardium by ultrasound-targeted microbubble destruction. *Ultrasonics*. 2012; 52:281–286. [PubMed: 21937069]
208. Zhou L, Dong K, Chen Z, Ren J, Qu X. Near-infrared absorbing mesoporous carbon nanoparticle as an intelligent drug carrier for dual-triggered synergistic cancer therapy. *Carbon*. 2015; 82:479–488.
209. Zhou B, Li D, Qian J, Li Z, Pang P, Shan H. MR tracking of SPIO-labeled mesenchymal stem cells in rats with liver fibrosis could not monitor the cells accurately. *Contrast Media Mol Imaging*. 2015; doi: 10.1002/cmml.1650
210. Zhou P, Xia Y, Cheng X, Wang P, Xie Y, Xu S. Enhanced bone tissue regeneration by antibacterial and osteoinductive silica-HACC-zein composite scaffolds loaded with rhBMP-2. *Biomaterials*. 2014; 35:10033–10045. [PubMed: 25260421]
211. Zhu Y, Shi J, Chen H, Shen W, Dong X. A facile method to synthesize novel hollow mesoporous silica spheres and advanced storage property. *Microporous Mesoporous Mater*. 2005; 84:218–222.

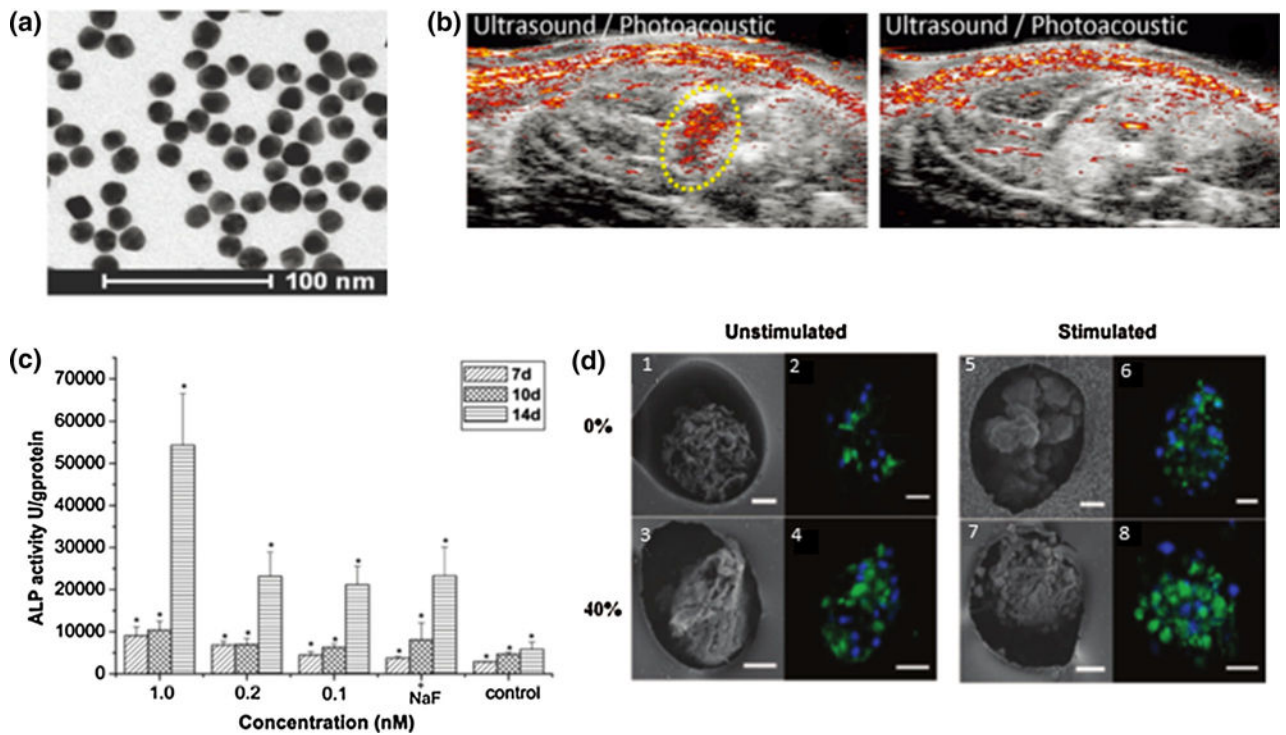


**Figure 1.**

(a) TEM image of 20 nm gold nanospheres.<sup>126</sup> (b) *In vivo* PA/US images of MSCs labeled with 20 nm AuNSs. The left panel is the treatment group, injected with labeled MSCs, and the right panel is the control, no injection.<sup>126</sup> (c) Gold nanoparticles can stimulate osteogenic differentiation, as increased AuNP concentrations lead to higher ALP activity.<sup>198</sup> (d) Cardiomyocytes seeded in scaffolds with AuNPs and treated with electrical stimulation lead to the highest connexin-43 expression, indicated by green fluorescence. (1, 2, 5, and 6) contain no thiol/(hydroxyethyl)methacrylate (HEMA) whereas (3, 4, 7, and 8) contain 40% thiol/HEMA, providing sites for AuNP growth. The left panel was unstimulated and the right panel was electrically stimulated.<sup>201</sup>

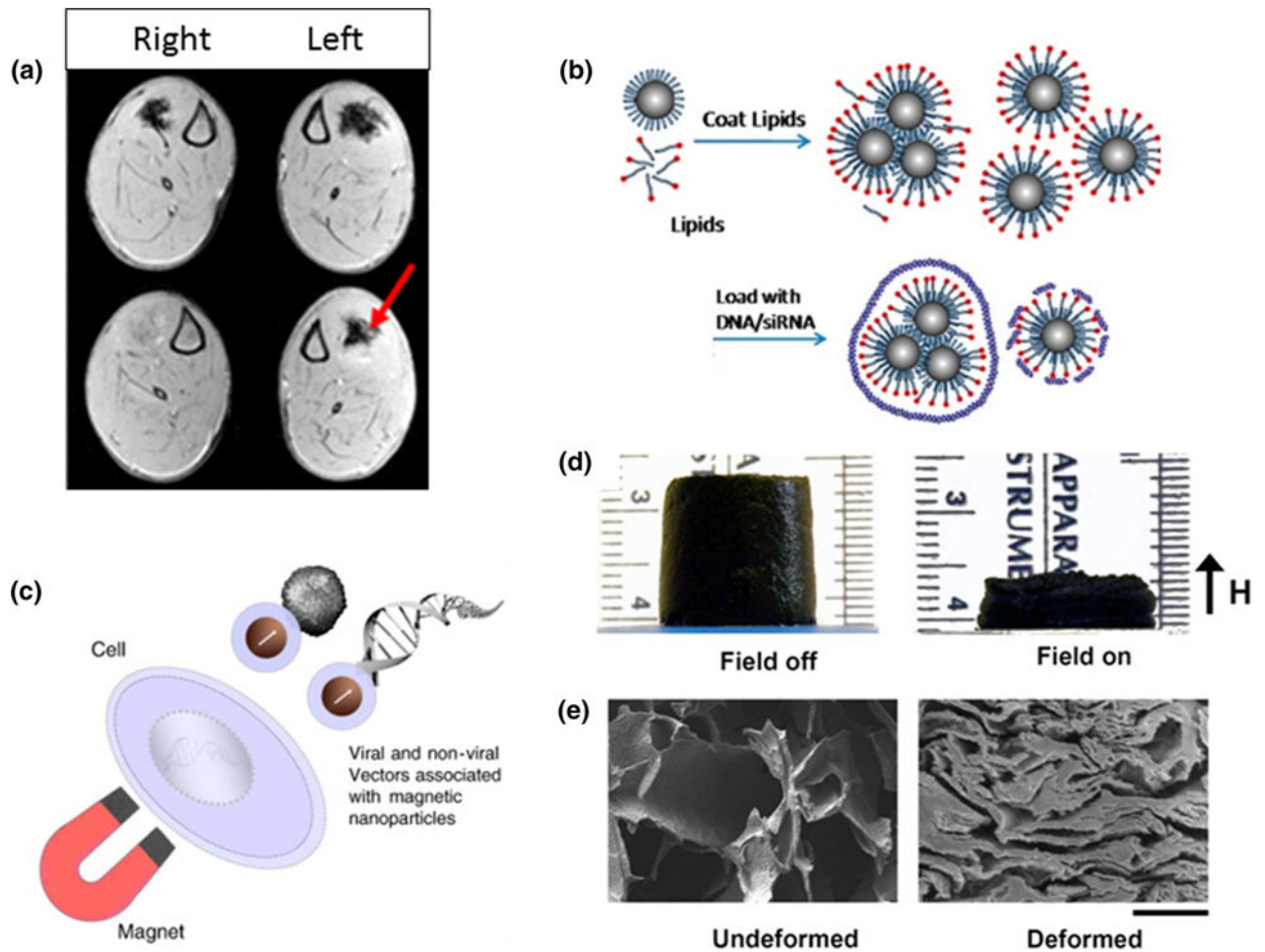


**Figure 2.**

(a) MRI shows *in vivo* accumulation and retention of IONP-containing platelets when a magnet is positioned on the left leg of the animal.<sup>167</sup> (b) Nucleic acids can be loaded on lipid-coated IONP for gene delivery applications.<sup>77</sup> (c) Magnetofection principle increases gene delivery efficiency by pulling the vectors and target cells together.<sup>142</sup> (d) A macroporous ferrogel is deformed when an external magnetic field is applied. (e) SEM images show a freeze-dried macroporous ferrogel in undeformed and deformed states (Scale bar = 500  $\mu\text{m}$ ).<sup>205</sup>

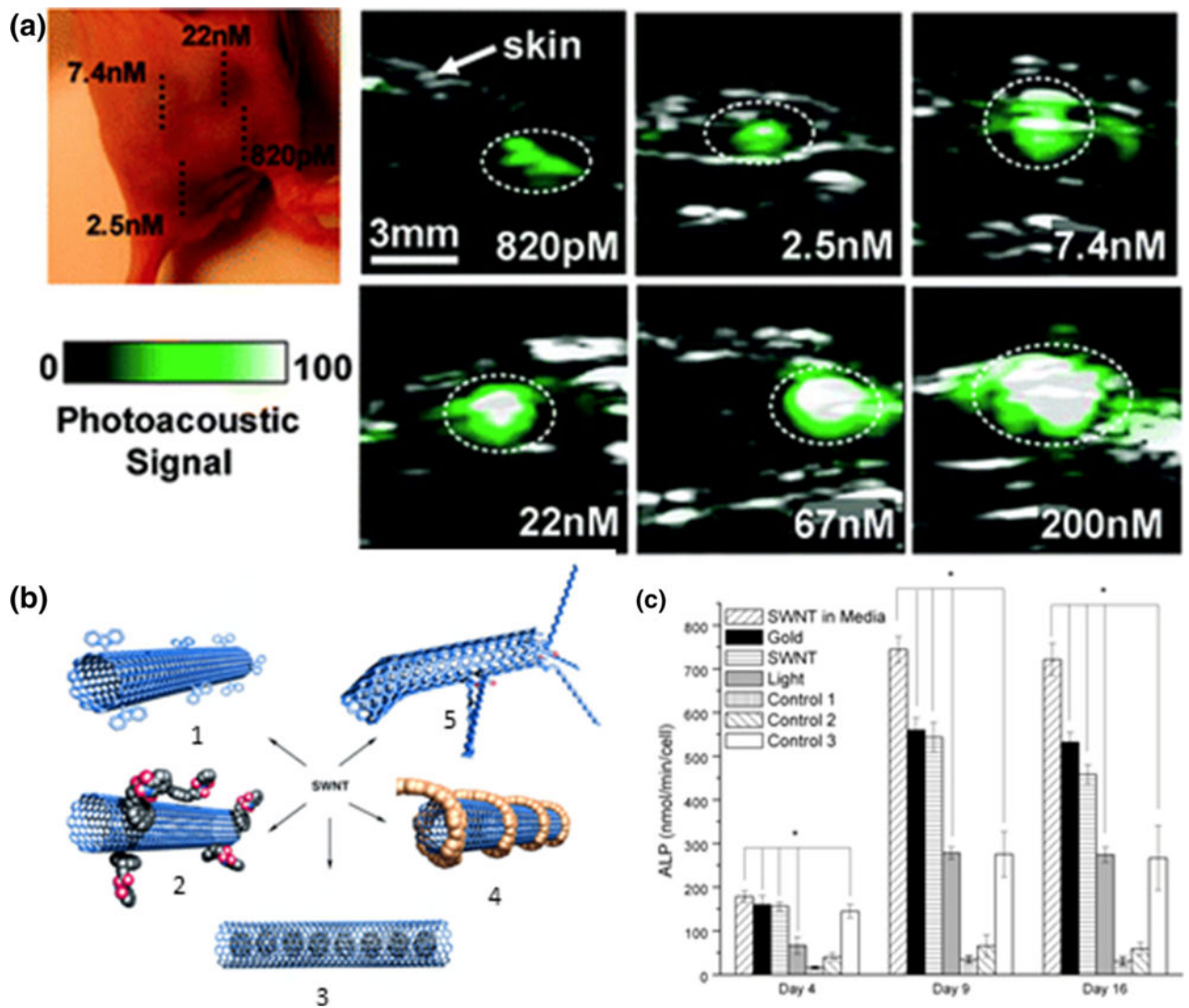


**Figure 3.**

(a) *In vivo* photoacoustic imaging of CNTs conjugated with ICG demonstrate high sensitivity. The PA signal increases linearly with CNT concentration.<sup>203</sup> (b) Schematic of different CNT functionalization methods for therapeutic delivery: (1) covalent sidewall functionalization, (2) non-covalent adsorption, (3) entrapment, (4) non-covalent wrapping, (5) defect-group functionalization.<sup>69</sup> (c) Depiction of irradiation effects in conjunction with CNTs and gold nanoparticles. CNTs incubated with MSCs and irradiated showed the biggest increase in ALP production. CNTs and gold nanoparticles adjacent to MSCs and irradiated showed more ALP production over controls without particles, but also irradiated.<sup>58</sup>

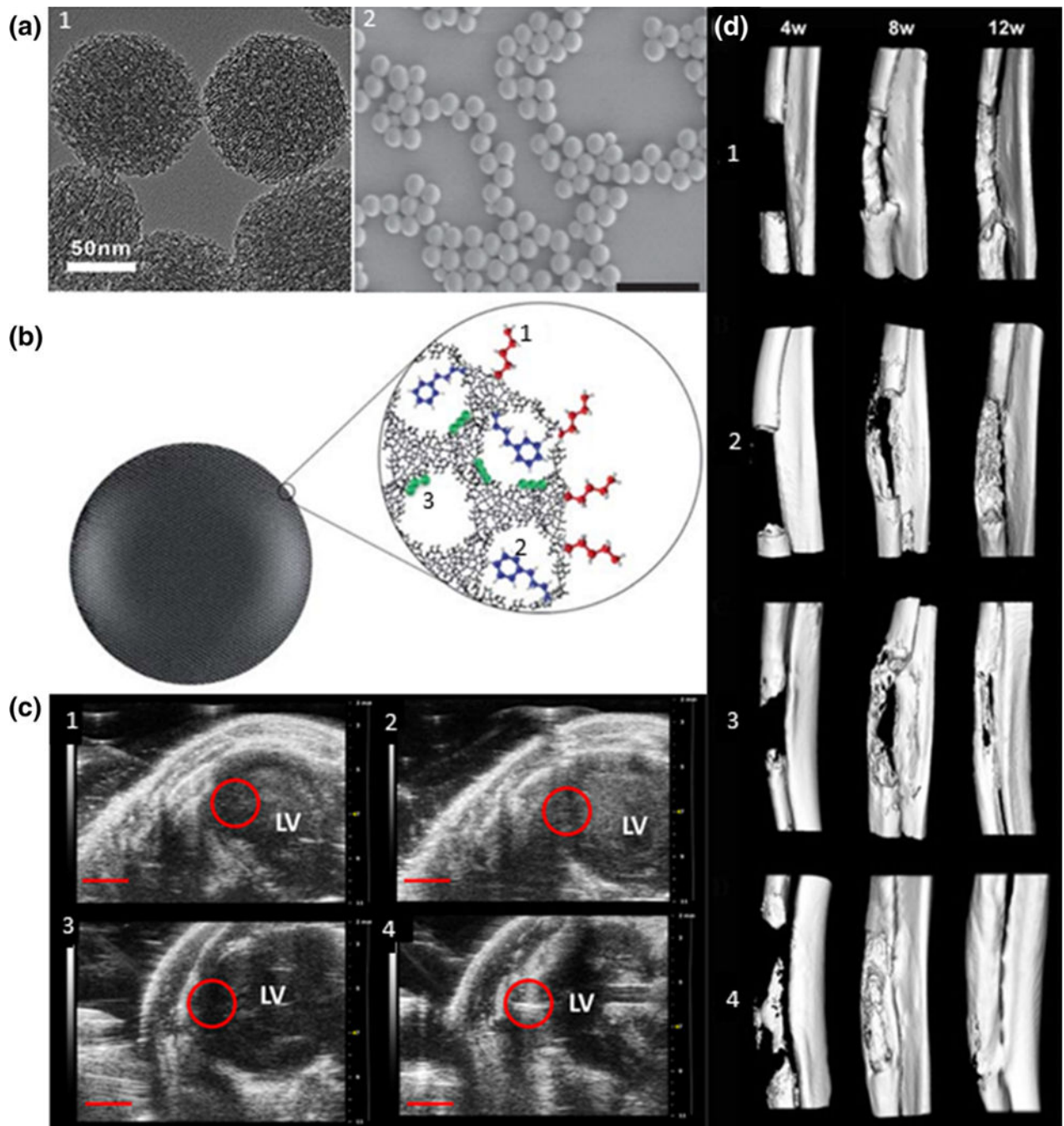


**Figure 4.** (a) (1) TEM of MSNs,<sup>28</sup> (2) SEM of SiNPs, (Scale bar = 1  $\mu\text{m}$ ).<sup>183</sup> (b) Functionalization of MSNs: (1) outer surface, (2) pore entrances, (3) inner walls.<sup>160</sup> (c) Micro-CT reconstructed images at 4, 8, and 12 weeks after implantation of (1) zein, (2) zein-HACC, (3) zein-S20, (4) zein-HACC-S20 scaffold. S20 is a type of MSN.<sup>210</sup> (d) In vivo US echogenicity of injected MSNs-labeled MSCs. (1) and (3) are pre-injection, (2) and (4) are post-injection. (2) is control and (4) is injection of 500,000 labeled MSCs.<sup>88</sup>

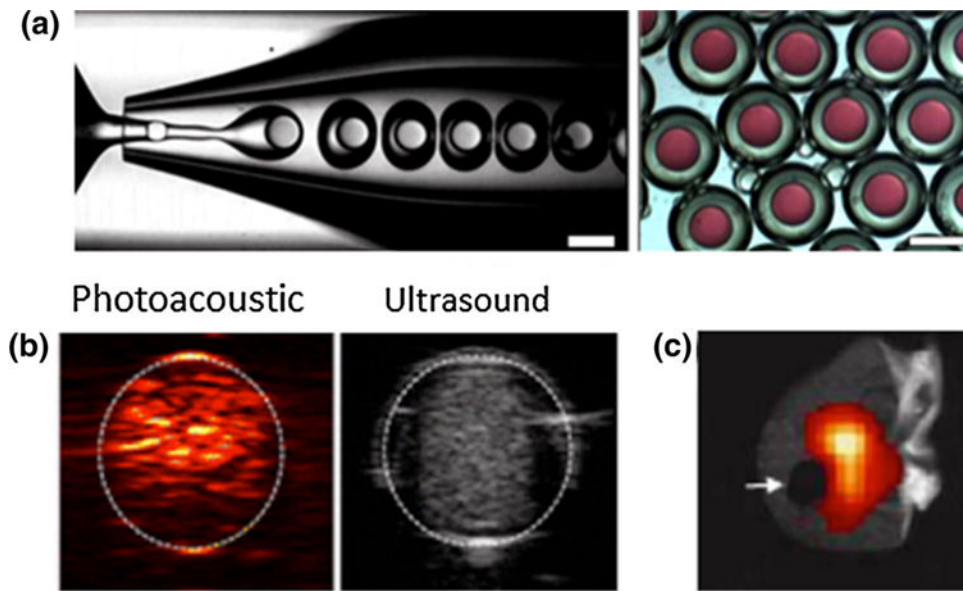


**Figure 5.** (a) Microfluidic synthesis of double emulsion PFCp microdroplets containing a model hydrophilic agent (red) (Scale bar = 200  $\mu\text{m}$ ).<sup>45</sup> (b) *In vitro* images of ICG-loaded PFCp nanodroplets that show PA and US contrast upon irradiation.<sup>63</sup> (c) Clipped mouse ear (arrow) shows how PFCps hone to the site of injury/inflammation and can be visualized with  $^{19}\text{F}$  MRI.<sup>76</sup>

TABLE 1

Summary of MIRA characteristics and applications.

| Agent      | Shape  | Synthesis methods  | Biocompatibility  | Imaging modalities  | Common Applications  | Disadvantages   |
|------------|--|--|---|---|--|---|
| AuNPs      | Wide range and choice depends on application | Spheres: citrate reduction and Brust-Schiffrin<br>Cages: galvanic replacement<br>Rods: use of capping agents (i.e. CTAB) <sup>38,192</sup> | High: bioinert, cytocompatible and nontoxic in short-term studies. Concerns with long-term effects <sup>147</sup> | X-ray/CT, PA imaging, and optical imaging                       | Cell tracking using PA imaging, drug or biomolecule delivery   | High cost and non-degradable leading to long-term toxicity, clearance issues, contrast agent transfer |
| IONPs      | Mainly spherical                             | Chemical co-precipitation, sol-gel reaction, precipitation in microemulsions<br>Hydrothermal reaction, pyrolysis <sup>60</sup>             | High: when coated with polymers and polysaccharides (e.g. dextran), some types have FDA-approval <sup>187</sup>   | MRI, combined MRI-nuclear imaging, magneto-motive               | Cell tracking and transport, gene delivery, magnetic scaffolds | Negative MRI contrast, contrast agent transfer, high cost and time consuming MRI                      |
| CNTs       | Single or multiple walled tubes              | Chemical vapor deposition, arc-discharge, laser <sup>65</sup>  | Medium: upon appropriate functionalization. Concerns over non-degradability <sup>55,65</sup>                      | Optical imaging, MRI, and PET                                   | Scaffold enhancers, cell tracking                              | Can affect SC proliferation and differentiation, do not degrade                                       |
| SINPs/MSNs | Spheres, hexagonal cylinders                 | Stöber Method, reverse microemulsion, evaporation-induced self-assembly <sup>171</sup>   | High: low cytotoxicity for nano-sized particles   | US and PET, MRI, or fluorescence by addition of contrast agents | Scaffold enhancers, drug delivery                              | Large size, potential to leak, additional contrast agents necessary for alternative imaging methods   |
| PFCps      | Nano or micron sized spheres                 | Emulsion techniques, microfluidics <sup>45,190</sup>   | High: PFCs are inert and are rapidly cleared <sup>150,190</sup>   | US, MRI, PA imaging   | Drug, gene or gas delivery                                     | Short lifetimes, large size of micro particles  |